TFAP2 transcription factors are regulators of lipid droplet biogenesis

Cameron C Scott[1], Stefania Vossio[1], Jacques Rougemont[2], Jean Gruenberg[1,3]

1. Department of Biochemistry, University of Geneva, 30 quai Ernest Ansermet
1211 Geneva 4, Switzerland
2. Department of Theoretical Physics, University of Geneva, 24 quai Ernest Ansermet
1211 Geneva 4, Switzerland

3. To whom correspondence should be addressed: jean.gruenberg@unige.ch

Abstract

How trafficking pathways and organelle abundance adapt in response to metabolic and physiological changes is still mysterious, although a few transcriptional regulators of organellar biogenesis have been identified in recent years. We previously found that the Wnt signaling directly controls lipid droplet formation, linking the cell storage capacity to the established functions of Wnt in development and differentiation. In the present paper, we report that Wnt-induced lipid droplet biogenesis does not depend on the canonical TCF/LEF transcription factors. Instead, we find that TFAP2 family members mediate the pro-lipid droplet signal induced by Wnt3a, leading to the notion that the TFAP2 transcription factor may function as a "master" regulator of lipid droplet biogenesis.

Introduction

Cellular adaptation to a changing local environment is imperative for survival and proliferation. This is effected through a collection of sensing and signalling pathways that integrate information about the local environment and induce the requisite changes in various cellular programs that control organelle abundance and function, through multiple routes, including the modulation of transcription. In recent years, several transcriptional 'master regulators' of organellar biogenesis have been reported for mitochondria (Jornayvaz and Shulman, 2010), autophagosomes (Kang et al., 2012, Chauhan et al., 2013) and lysosomes (Sardiello et al., 2009). While the functional details of this control are still under investigation, coordinated transcriptional control of specific organelles is an emerging theme in cell biology.

Lipid droplets are the primary storage organelle for neutral lipids in the cell (Meyers et al., 2017). Intriguingly, the number and nature of these organelles vary greatly, both over time within a cell, and between cell types (Thiam and Beller, 2017). While a major function of lipid droplets is clearly as the storehouse of triglycerides and sterol esters, the diversity and variation of this organelle likely reflect the number of reported alternate functions of lipid droplets such as regulation of inflammation, general metabolism, and host-pathogen interplay (Barisch and Soldati, 2017, Melo and Weller, 2016, Konige et al., 2014). Despite the recognized importance of this organelle in health and disease, little is known of the signalling systems or proximal transcriptional regulators that control lipid droplet biogenesis, function and turnover in cells.

Recently, we used genome-wide, high-content siRNA screens to identify genes that affect cellular lipids. This analysis revealed that the Wnt ligand can potently stimulate lipid droplet accumulation in multiple cell types (Scott et al., 2015). In this paper, we report that the biogenesis of lipid droplets induced by Wnt signaling does not depend on the canonical TCF/LEF transcription factors. Our data show that the pro-lipid droplet signal induced by Wnt3a is mediated by members of the TFAP2 family of transcription factors. We thus conclude that TFAP2 may function as a “master” regulator of lipid droplet biogenesis.

Results

Wnt-induced lipid droplet formation could be conveniently visualized using BODIPY, which accumulated in lipid droplets (Fig 1A) and (Scott et al., 2015), and quantified by automated

65 microscopy (Fig 1B, and all subsequent figures). Similarly, accumulation of lipid droplets in
66 Wnt-treated cells could also be revealed in cells expressing the lipid droplet protein PLIN1a
67 tagged with the GFP (Fig. 3 - Fig.Sup. 1C and F; quantification in D and G, respectively) or
68 by direct determination of triglyceride and cholesteryl ester amounts (Fig. 3 - Fig.Sup. 1) and
69 (Scott et al., 2015). In our previous work, we had observed that Wnt stimulates lipid droplet
70 accumulation through upstream elements of the Wnt signalling pathway, including the
71 canonical surface receptors and adenomatous polyposis coli (APC), a component of the
72 destruction complex (Scott et al., 2015). This role of Wnt is well in-line with the established
73 functions of Wnt signalling in the control of cellular metabolism, including carbohydrate,
74 protein and lipid (Prestwich and Macdougald, 2007, Sethi and Vidal-Puig, 2010, Ackers and
75 Malgor, 2018). Therefore, to further characterize the signalling cascade leading to the
76 accumulation of lipid droplets after Wnt addition, we tested the key components from the
77 canonical Wnt signalling pathway for a role in lipid droplet regulation, starting with the core
78 enzyme of the destruction complex, GSK3B (Fig. 1A-C). We found that overexpression of
79 both the wild-type, and the constitutively-active S9A (Stambolic and Woodgett, 1994) mutant
80 of GSK3B were capable of attenuating lipid droplet accumulation in response to Wnt3a-
81 treatment (Fig. 1A-B), consistent with the function of GSK3B activity as a negative regulator
82 of Wnt signalling. Further, siRNAs to GSK3B were sufficient to induce lipid droplet
83 accumulation (Fig. 1A,C) — much like we had shown after gene silencing of APC, another
84 member of the destruction complex (Scott et al., 2015).
85
86 We next investigated the possible role of the downstream targets of the Wnt pathway at the
87 transcription level. Surprisingly, siRNAs to TCF/LEF transcription factors relevant in
88 canonical Wnt signalling, failed to affect lipid droplet accumulation - and yet there is no
89 doubt that lipid droplet accumulation in response to Wnt3a is transcriptionally mediated.

Indeed, the expression of SOAT1 and DGAT2, which encode key-enzymes of lipid droplet formation, increased in response to Wnt3a-treatment (Scott et al., 2015). In addition, silencing these genes inhibited lipid droplet accumulation in response to Wnt3a, most potently in combination with each other (Fig. 1D; silencing efficiency Fig. 1 - Fig.Sup. 1B), or with specific inhibitors to DGAT1 or SOAT (Fig. 1E, Fig. 1 - Fig.Sup. 1A). Finally, Wnt3a-induced lipid droplets were decreased after treatment with the general inhibitor of transcription Actinomycin D (Fig. 1E). While these data altogether confirmed that the Wnt pathway was mediating the pro-lipid droplet signal, our inability to link lipid droplet induction to TCF/LEF led us to consider the possibility that a branching signalling path, under the control of GSK3B and/or ß-catenin but not the canonical Wnt transcription factors TCF/LEF, was inducing the accumulation of lipid droplets in cells. To explore this possibility, we initiated several parallel and complementary systems-level analyses with the aim to identify the transcriptional regulators proximal to lipid droplet biogenesis.

To better understand the nature of the pro-lipid droplet signal induced by Wnt, we revaluated the involvement of individual components of the Wnt signalling pathway in the induction of lipid droplet accumulation. First, we tested the ability of each of the 19 human Wnt ligands to induce lipid droplet accumulation in L Cells by transfection and autocrine or paracrine induction of the Wnt pathway (Fig. 1F-G). Wnt ligands displayed a broad, but not universal capacity to induce lipid droplet accumulation that paralleled both their evolutionary pedigree (Fig. 1F), and previously reported abilities to activate canonical Wnt signalling as measured by a TCF/LEF reporter system (Najdi et al., 2012). This confirmed that the pro-lipid droplet signal was indeed transiting, at least initially, through canonical Wnt signalling components.

To systematically assess the involvement of the remaining components of the Wnt pathway for involvement in the lipid droplet response, we performed a targeted screen for factors influencing lipid droplet accumulation using a library of 73 compounds selected for known interactions with elements of the Wnt pathway (see Methods). We tested the library in both, Wnt3a-stimulated conditions to assess any inhibitory activity of lipid droplet accumulation, and unstimulated conditions to identify compounds with the ability to induce the phenomenon (Fig. 1 – Source Data 1). Indeed, treatment with several compounds reported to activate the Wnt pathway induced lipid droplet accumulation, such as BML-284 (activator of ß-catenin (Liu et al., 2005)), doxorubicin (activator of Wnt signalling (Dai et al., 2009)), and forskolin (activation via PKA-Wnt crosstalk (Zhang et al., 2014)) (Fig. 1H-I). Conversely, known inhibitors of the pathway such as Tricostatin A (epigenetic regulator of DKK1 (Vibhakar et al., 2007)) hexachlorophene (ß-catenin inhibitor (Park et al., 2006)), and niclosamide (inducer of LRP6 degradation (Lu et al., 2011)) significantly decreased the appearance of lipid droplets in response to Wnt3a (Fig. 1H-I).

While these data certainly confirm the role of Wnts in regulating lipid droplets, they did not reveal the pathway linking the Wnt destruction complex to the transcriptional changes we observed (Fig. 1A-E, (Scott et al., 2015)). Given these results, and the large number of ß-catenin-independent targets of the destruction complex (Kim et al., 2009), we initiated several strategies to identify candidate regulators, in particular the proximal transcription factors directly upstream from lipid droplet biogenesis. Our aim was to identify factors linked to Wnt signalling and to characterize the signalling pathway from ligand-stimulation to lipid droplet accumulation.

We first started by taking the subset of genes annotated as 'transcription factor activity' (GO:0000988) from our primary genome-wide siRNA screen data (Scott et al., 2015) to identify transcription factors that influenced cellular cholesterol levels in the cell (Fig. 2 - Fig.Sup. 1A; Fig. 2 – Source Data 1). While several of these candidates have well established roles in regulating general proliferation (i.e. MACC1, JDP2, SP3, TP53, ZNF217, TAF1), or links to the WNT pathway in keeping with our findings (i.e. GLI3, SIX2, SOX9, FOXK2, BARX1), we were particularly interested in identifying candidates with reported functions in lipid metabolism. The latter subset included ARNT2, STAT3, KDM3A, ATF5, KLF5, KLF6 and members of the TFAP2 (AP-2) transcription factor family (see below).

As a second approach to search for candidate transcriptional regulators of lipid droplets we compared existing transcriptome data of Wnt3a-treated cells with that of other conditions known to induce the accumulation of lipid droplets in tissue culture cells. It is well-established the formation of lipid droplets is stimulated artificially by the addition of exogenous fatty acids (Martin and Parton, 2006), and the process has been studied at the transcriptional level in multiple studies. We therefore combined our Wnt3a gene array data (Scott et al., 2015) with three published datasets of mRNA levels after treatment of cells with fatty acids or knockout of lipid droplet regulatory factors (Li et al., 2010, Lockridge et al., 2008, Shaw et al., 2013). Our rationale was to identify the relevant transcription factors required for the induction of lipid droplet biogenesis by inferring from the expression data what is the common set of transcription factors active in response to Wnt3a and/or to the modulation of lipid droplets by fatty acid treatment or gene knockout. This analysis involved testing for over-representation of genes annotated to be regulated by a specific transcription factor in the set of the most perturbed genes after either treatment. Wnt3a-stimulation influenced a larger number of transcriptional regulators (172) as compared to lipid droplet

modulation (91), but the vast majority of this subset (>75%) were also changed by Wnt3a (Fig. 2 - Fig.Sup. 1B). With this approach, we found that many candidate transcription factors known to function in both lipid metabolism and adipogenesis were influenced by Wnt3a-treament and fatty acid perturbation (Fig. 2 – Source Data 2), including TFAP2A (p-value Wnt3a treatment: 3.5×10^{-9}; p-value fatty acid perturbation: 4.8×10^{-4}).

As a third systems-level approach, we undertook a direct examination of the promotor regions of annotated lipid droplet proteins as was used by Sardiello and colleagues to identify the transcription factor TFEB and the CLEAR element as master regulators of lysosome biogenesis (Sardiello et al., 2009). We collected and examined the upstream promoter sequences for the 145 proteins annotated as 'Lipid Droplet' (GO:0005811; Fig. 2 – Source Data 3) and tested for over-represented sequence motifs. Among the most enriched motifs in the upstream promotor region of lipid droplet genes were motifs identified as TFAP2A (pValue: 9.0×10^{-3}) and TFAP2C (pValue: 1.8×10^{-5}) binding sites (Fig. 2 - Fig.Sup. 2A). Further analysis revealed that 74 of the 'Lipid Droplet' proteins contained at least one of the TFAP2A or TFAP2C annotated binding sites (Fig. 2 - Fig.Sup. 2B, Fig. 2 - Source Data 3) which were generally present within the first few hundred base-pairs from the start site (Fig. 2 - Fig.Sup. 2C).

The TFAP2 (AP-2) family of basic helix-span-helix transcription factors have been long recognized to play key roles during development (Eckert et al., 2005). Yet, little else is known regarding their function in adult animals where these proteins are expressed, although various TFAP2 homologs have been linked to tumour progression in cancer models (Eckert et al., 2005, Li and Dashwood, 2004, Li et al., 2009). The family consists of five proteins in human and mouse, and are thought to form homo- and heterodimers that bind to similar

promotor sequences albeit with different affinities (Eckert et al., 2005). Given our observation that downstream genes known to be regulated by TFAP2 family members change in response to Wnt3a (Fig. 2 - Fig.Sup. 1B), that the silencing of TFAP2 genes can regulate cholesterol amounts in cells (Fig. 2 - Fig.Sup. 1A), and that TFAP2 consensus sites are over-enriched in the promoter sequences of genes encoding for lipid droplet proteins (Fig. 2 - Fig.Sup. 2A), we began to suspect that TFAP2 proteins mediate the pro-lipid droplet signal induced by Wnt3a. This notion was further buttressed by previous studies showing that TFAP2A directly interacts with both ß-catenin and APC (Li et al., 2009, Li et al., 2015) making this family of transcription factors our leading candidate for mediating the pro-lipid droplet signalling activity of Wnt3a.

To gain a detailed description of the transcriptional changes in the context of TFAP2, Wnt and lipid droplets, we performed an RNAseq determination of mRNA levels in cells treated with Wnt3a for short times (2h and 6h) with the aim to identify early factors of the transcriptional control relevant for lipid droplet biogenesis. As expected, a pathway analysis of the most responsive genes at 2h found over-representation of terms related to mRNA processing, DNA binding and transcriptional regulation (Fig. 2A), consistent with the expected nature of the early Wnt3a-responsive genes. By 6h post-Wnt3a treatment, transcriptional regulators were still over-represented, but additional terms reflecting downstream effector pathways were present, including those related to glucose metabolism and endosomal trafficking, as well as fatty acid and cholesterol related genes (Fig. 2A) consistent with our previous findings (Scott et al., 2015). Indeed, the RNAseq analysis found that SREBF1 (Sterol Regulatory Element Binding Transcription Factor 1) mRNA levels were the most decreased of any transcription factor (0.60 of control) at the later time point (Fig. 2B).

Intriguingly, the most upregulated transcription factor at early times was DDIT3 (DNA Damage Inducible Transcript 3, also known as CHOP) — and increased DDIT3 could readily be detected at the mRNA and protein level (Fig. 2 - Fig.Sup. 3A-B). This member of the CCAAT/enhancer-binding (CEBP) protein family is a potent and direct inhibitor of SREBF1 transcription (Chikka et al., 2013) and a known regulator of cellular lipid metabolism. While this interaction may contribute to the decrease in cellular free cholesterol and the downregulation of cholesterol metabolic enzymes after Wnt3a treatment (Fig. 2A, (Scott et al., 2015)), overexpression of constitutively-active SREBF1 truncations (Shimano et al., 1997) had essentially no effect on the formation of lipid droplets, whether Wnt3a was present or not (Fig. 2 - Fig.Sup. 4A) despite activating known target genes involved in cholesterol metabolism (Fig. 2 - Fig.Sup. 4C). Neither did treatment with the S1P/SREBF1 inhibitor PF-429242 (Hawkins et al., 2008) (Fig. 2 - Fig.Sup. 4B) in either Wnt3a-stimulated, or naïve conditions. These observations suggest that while relevant to the observed changes in cellular cholesterol homeostasis generated by Wnt3a, putative DDIT3-induced changes in SREBF1 expression have no significant role in lipid droplet accumulation in response to Wnt3a.

Along with DDIT3 and SREBF1, our list of early Wnt3a-responsive transcription factors includes several that have known functions in regulating cellular lipid homeostasis such as CEBPB and CEBPE, KLF5, KLF10, PPARG, MLXIPL, and PER2. Our list also included the TFAP2 family member TFAP2C, which our datamining strategies had already identified as involved in lipid homeostasis, and as a candidate transcription factor controlling lipid droplet biogenesis. In fact, 6h post-Wnt3a stimulation TFAP2C (1.72-fold) was among the most upregulated transcription factors (Fig. 2B).

Given that our datamining efforts identified TFAP2 family members as putative transcription factors regulating lipid droplet proteins and that TFAP2C was among the most upregulated transcription factors in response to Wnt3a (Fig. 2B), we next investigated whether TFAP2 family members played a direct role in regulating lipid droplets. To this end, we tested the ability of TFAP2A to directly bind to the promotor region of known lipid droplet, and lipid metabolic genes containing a predicted TFAP2 consensus site by ChIP-PCR (Fig. 2C), including the enzymes ACSL3, ACSL4, AGPAT2, AGPAT3, LPCAT2, and MGLL, and the lipid droplet resident proteins PLIN3, PLIN4, PNPLA2, and PNPLA3 (Meyers et al., 2017, Barneda and Christian, 2017). Indeed, we found that the TFAP2A protein was able to bind the upstream promotor of all the genes we tested, supporting the notion that expression was controlled by TFAP2 family members. Next, we tested whether Wnt3a retained the ability to induce lipid droplets after TFAP2 depletion by RNAi. While knock-down of either TFAP2A or TFAP2C had no or only a modest effect, tandem silencing of both homologs produced a marked reduction in the number of lipid droplets present in cells in response to Wnt3a (Fig. 3A-B; knock-down efficiency Fig. 3 - Fig.Sup. 2A) and markedly decreased the amounts of cholesteryl esters (Fig. 3 - Fig.Sup. 1A). In keeping with these findings, these siRNA treatments diminished the mRNA levels of SOAT1, a key enzyme proximal to the production of lipid droplets (Fig 3C) that mediate the production of cholesteryl esters (Chang et al., 2001). These observations indicate that TFAP2 family members exhibit complementary functions.

As an alternative approach, we used CRISPR/Cas9 gene knockout to generate HeLa-MZ cells clones lacking TFAP2A (Fig. 3D-E). While tandem depletion by RNAi was necessary to reduce lipid droplet production after Wnt3a addition in L Cells, two knockout clones of TFAP2A demonstrated a complete lack of change in lipid droplet number after Wnt3a

stimulation (Fig. 3D-E; and see Fig. 3 - Fig.Sup. 1C-D) and failed to accumulate triglycerides (Fig. 3 - Fig.Sup. 1B). The ability of Wnt to induce LD formation could be rescued upon TFAP2A re-expression (Fig. 4 - Fig.Sup. 1D), demonstrating that the inhibition observed in knock-out cells was not caused by some off-target or indirect effect of the treatment. Together, these results imply that TFAP2A/TFAP2C are necessary for mediating the pro-lipid droplet signal of the Wnt pathway.

We next sought to determine if the TFAP2 family is sufficient for the induction of lipid droplets. For this, we fused full-length TFAP2A, TFAP2B, and TFAP2C to mCherry and overexpressed these as exogenous chimeras. As transcription factors the TFAP2 family members function in the nucleus, the mCherry-tagged TFAP family members exhibited a somewhat heterogeneous distribution between cytoplasm and nuclei, presumably because of variations in expression levels. Impressively, the number of lipid droplets per cell increased with increased nuclear localization of each TFAP2 family member (Fig. 3H; (Fig. 3 - Fig.Sup. 1F-G); relative overexpression Fig. 3 - Fig.Sup. 2B), and, in cells with TFAP2 nuclear localization, the expression of each family member was clearly sufficient to cause lipid droplet biogenesis (Fig. 3F-G). Moreover, the expression of TFAP2C was also able to trigger the expression of lipid droplet enzymes (Fig. 3I) and accumulation of cholesterol esters and triglycerides (Fig. 3 - Fig.Sup. 1E), further supporting the notion that TFAP2 family members function as transcriptional regulators of lipid droplet biogenesis.

In totality, these findings demonstrate TFAP2A, TFAP2B and TFAP2C are sufficient to induce biogenesis of lipid droplets when expressed in cells, and members of the TFAP2 family are required to mediate the accumulation of lipid droplets seen in response to Wnt-stimulation. This finding is in keeping with a previous report that targeted overexpression of

TFAP2C in mouse liver induced steatosis, accumulation of fat, and eventual liver failure (Holl et al., 2011), and given the enrichment in TFAP2 binding sites in lipid droplets proteins (Fig. 2 - Fig.Sup. 2), implicate the TFAP2 family as central regulators of lipid droplet biogenesis.

Given our observation that TFAP2C expression correlates with DDIT3 expression in cells after Wnt3a treatment (Fig. 2B), we investigated the role of DDIT3 in control of lipid droplets. We started by examining the promotor region of the transcription factors whose mRNA levels were impacted by Wnt3a-treatment (Fig. 2B) for reported DDIT3::CEBPA consensus sites (Ubeda et al., 1996). Intriguingly, not only did we find such a site upstream of the TFAP2C gene, but there was a DDIT3::CEBPA consensus site in 7 out of the 10 lipid-related transcription factors identified in our RNAseq (Fig. 4 - Fig.Sup. 1A), a 1.8-fold enrichment over the frequency in the total Wnt3a-influenced transcription factor set. This lends further support for the view of DDIT3 as an important transcriptional regulator of lipid homeostasis in cells (Chikka et al., 2013).

To address this notion directly, we next tested whether DDIT3 itself was able to influence both TFAP2 family members, and the number of lipid droplets in cells. Indeed, overexpression of DDIT3-mCherry chimera increased mRNA levels of lipid droplet enzymes, without much of an effect on lipid droplet coat proteins (Fig. 4A; relative overexpression Fig. 3 - Fig.Sup. 2D), with a concomitant increase in cholesteryl esters and triglycerides (Fig. 3 - Fig.Sup. 1B). Further, silencing of DDIT3 influenced the mRNA levels of many lipid metabolic genes including decreasing the levels of SOAT1 (Fig. 4B; knock-down efficiency Fig. 3 - Fig.Sup. 2C), as well as reducing cholesteryl ester accumulation (Fig. 3 - Fig.Sup. 1A) and lipid droplet accumulation (Fig. 4C) in response to Wnt3a. These

observations suggest that DDIT3 plays a regulatory role in lipid droplet biogenesis, presumably in concert with TFAP2.

We next tested the requirement of DDIT3 for the lipid droplet response directly by interfering with DDIT3 expression by both RNAi and CRISPR/Cas9. Silencing of DDIT3 expression diminished accumulation of lipid droplets both in response to Wnt3a stimulation (Fig. 4D; Fig. 4 - Fig.Sup. 1B; Fig. 3 - Fig.Sup. 1C-D), and after silencing of APC (Fig. 4 - Fig.Sup. 1B), an alternative strategy previously shown to be sufficient to induce lipid droplets (Scott et al., 2015). Wnt3a-induced increase in triglycerides was also ablated in these CRISPR clones (Fig. 3 - Fig.Sup. 1B). Further, knock-out clones lacking DDIT3 were completely non-responsive to Wnt3a with regards to lipid droplet number (Fig. 4D). Much like with TFAP2A, DDIT3 re-expression in knock-out cells rescued Wnt-induced LD formation (Fig. 4 - Fig.Sup. 1D), demonstrating that the inhibition observed in KO cells was not due to some off-target effects. In the context of the significant increase in DDIT3 message and protein (Fig. 2 - Fig.Sup. 3), these results suggest that induction of DDIT3 transcription in response to Wnt3a is necessary for lipid droplet biogenesis.

Given that the presence of DDIT3 was necessary to convey the pro-lipid droplet signal, we next tested whether over-expression of the transcription factor is sufficient to induce lipid droplet accumulation. As with TFAP2, overexpression of mCherry-tagged fusions of DDIT3 was sufficient to increase lipid droplet numbers (Fig. 4E; Fig. 4 - Fig.Sup. 1C; Fig. 3 - Fig.Sup. 1F_G) as well as cholesterolyl esters and triglyceride levels (Fig. 3 - Fig.Sup. 1E) in transfected cells as compared to the control. In total, these data suggest that in addition to regulation of cholesterol metabolism (Chikka et al., 2013), DDIT3 may function as a more global regulator of cellular lipid homeostasis in part through regulation of the TFAP2 family

of transcription factors. In an attempt to clarify the relationship between DDIT2 and TFAP2A, we tested whether TFAP2A overexpression restored Wnt-dependent LD formation in DDIT3 knock-out cells and vice versa (Fig. 4 - Fig.Sup. 1D). While TFAP2A did not rescue DDIT3 knock-out cells, DDIT3 expression was able to restore LD formation in TFAP2A knock-out cells. Although future work will be required to determine the precise functions of DDIT3, it is tempting to speculate that TFAP2A drives DDIT3 expression (or that DDIT3 responds lipid droplet accumulation). DDIT3 therefore, in addition to a direct inducer of lipid storage, might act as TFAP2A repressor — in line with the known repressor function of DDIT3 in SREBP expression (Chikka et al., 2013).

Discussion

In conclusion, our data show TFAP2 family members function to modulate expression of lipid droplet proteins and induce the accumulation of lipid droplets in cells. We found TFAP2C is necessary to potentiate the pro-lipid droplet signal induced by Wnt3a, and expression of TFAP2 family members is sufficient to induce lipid droplet accumulation in cells (Fig. 3).

Not only do these data support the view that the TFAP2 family of transcription factors can function as regulators of lipid droplet biogenesis, they provide insight into the transcriptional network directing changes in lipid homeostasis and the accumulation of lipid droplets in response to Wnt stimulation. Our data also provides further decoding of the known relationships between Wnt signaling and the control of cellular metabolism (Prestwich and

Macdougald, 2007, Sethi and Vidal-Puig, 2010, Ackers and Malgor, 2018). Finally, our observations indicate that, in addition to the canonical TCF/LEF transcriptional response, Wnt signalling via APC, GSK3, and ß-Catenin induces transcription-mediated lipid changes. These include decreased levels of SREBF1, which is likely to contribute to the observed reduction in total membrane cholesterol levels (Scott et al., 2015), and increased expression of DDIT3 and TFAP2, which triggers lipid droplet biogenesis with storage of cholesterol esters and triglycerides. These observations also lead to the notion that via TFAP2 transcription factors, Wnt exerts pro-proliferative effects in developmental and in pathological contexts by leading to the accumulation of lipid droplets.

In addition, Wnt3a has been recently identified as an intra-cell synchronizer of circadian rhythms in the gut, controlling cell-cycle progression, and the mRNA of Wnt3a itself exhibits circadian oscillations under the control of the master clock regulators Bmal1 and Per (Matsu-Ura et al., 2016). Given this function, it is tempting to speculate that Wnts serve a more general role as a mid- or long-range circadian signalling intermediates, linking lipid metabolism to the master transcriptional clocks that coordinate metabolic functions with the day-night cycle. Because of its circadian nature, and capacity to induce lipid droplet accumulation in a broad range of cells types, Wnts could serve as a fundamental signal for cells to store lipids during times when nutrients are expected to be in excess for later use during periods of rest or fasting.

Both lipid droplets enzymes (Solt et al., 2012), and the volume of lipid droplets themselves (Uchiyama and Asari, 1984), vary in a circadian fashion, which is completely consistent with a role as neutral lipid storage sites. TFAP2 binding sites are over-represented in the promotors of circadian-controlled genes (Bozek et al., 2009), suggesting that the Wnt/TFAP2

control of lipid droplets is one mechanism by which the daily storage of lipids in lipid droplets, and cellular lipid homeostasis itself, is coordinated. Further, targeted overexpression of TFAP2C induced the equivalent phenotype of steatosis in mouse liver (Holl et al., 2011), underscoring the role of TFAP2 proteins in the regulation of neutral lipid metabolism.

The Wnt pathway is also not the first developmental signalling pathway found to exert key regulatory functions in directing energy metabolism. The FOXA family of transcription factors, fundamental for early embryogenesis, play core roles in directing glucose metabolism (Friedman and Kaestner, 2006), while SOX17 has been shown to have additional, non-developmental functions regulating lipid metabolism in the liver of adult animals (Rommelaere et al., 2014). Given the overlapping requirement for a molecular queue to synchronize energy storage during both embryo development and daily metabolic activity, it is not surprising that some of these systems have evolved to serve dual roles in both biological contexts. These findings support the view that both Wnt signalling, and the TFAP2 family of transcription factors have important (and possibly linked) roles in development and circadian lipid metabolism of the cell.

Materials and Methods

Key resources table

Reagent type (species) or resource	Designation	Source or reference	Identifiers	Additional information
cell line (*Mus musculus*)	L Cells	American Type Culture Collection	Cat #: CRL-2648; RRID:CVCL_4536	PMID:14056989
cell line (*Mus musculus*)	L Wnt3A Cells	American Type Culture Collection	Cat #: CRL-2647; RRID:CVCL_0635	PMID:12717451
cell line (*Homo sapiens*)	HeLa-MZ	other		Clone of HeLa (American Type Culture Collection Cat#: CCL-2) provided by Prof. Lucas Pelkmans (University of Zurich)
cell line (*Homo sapiens*)	CRISPR DDIT3	this paper		
cell line (*Homo sapiens*)	CRISPR TFAP2A	this paper		
transfected construct (*Homo sapiens*)	GSK3B	Addgene	Cat #: 49491	
transfected construct (*Homo sapiens*)	GSK3BS9A	Addgene	Cat #: 49492	
transfected construct (*Homo sapiens*)	Wnt Project plasmid library	Addgene	Kit # 1000000022	
transfected construct (*Homo sapiens*)	pCMV-SREBP-1a(460)	American Type Culture Collection	Cat #: 99637	PMID:9062341
transfected construct (*Homo sapiens*)	pCMV-SREBP-1c(436)	American Type Culture Collection	Cat #: 99636	PMID:9062341

transfected construct (*Homo sapiens*)	pCMV-SREBP-2(468)	American Type Culture Collection	Cat #: 63452	PMID:9062341
transfected construct (*Homo sapiens*)	DDIT3-mCherry	this paper		
transfected construct (*Homo sapiens*)	mCherry-TFAP2A	this paper		
transfected construct (*Homo sapiens*)	mCherry-TFAP2B	this paper		
transfected construct (*Homo sapiens*)	mCherry-TFAP2C	this paper		
transfected construct (*Homo sapiens*)	V5-TFAP2A	this paper		
biological sample (*Bos taurus*)	Lipoprotein-depleted serum	PMID:13252080		
antibody	Rabbit anti-AP2 alpha; anti-TFAP2A	Abcam	Cat #: ab52222	
antibody	Mouse anti-CHOP (L63F7); anti-DDIT3	Cell Signaling	Cat #: 2895	
antibody	Mouse anti-V5 Tag	ThermoFisher Scientific	Cat #: R960-25	
recombinant DNA reagent	CRISPR Forward: DDIT3	Microsynth		CACCGGCACCTATATCTCATCCCC
recombinant DNA reagent	CRISPR Forward: TFAP2A	Microsynth		CACCGGAGTAAGGATCTTGCGACT

recombinant DNA reagent	CRISPR Reverse: DDIT3	Microsynth		AAACGACTGATCCAACTGCAGAGAC
recombinant DNA reagent	CRISPR Reverse: TFAP2A	Microsynth		AAACAGTCGCAAGATCCTTACTCC
recombinant DNA reagent	Primer Forward: ACSL3	Microsynth		TGAGCTCTCTTTGCTTGGTG
recombinant DNA reagent	Primer Forward: ACSL4	Microsynth		AAGGACATCCCGAAACACAC
recombinant DNA reagent	Primer Forward: AGPAT2	Microsynth		GGCCTAAGGCAAAAGGATGTG
recombinant DNA reagent	Primer Forward: AGPAT3	Microsynth		ACCCAAGCTCAGCAAGTCC
recombinant DNA reagent	Primer Forward: CTCF	Microsynth		GCCAGTCCAACCGGCTTATG
recombinant DNA reagent	Primer Forward: LPCAT2	Microsynth		AGGGGAAGTGGTTGCTCAATG
recombinant DNA reagent	Primer Forward: MGLL	Microsynth		GAACCCAGCTCAGTTCAGG
recombinant DNA reagent	Primer Forward: PLIN3	Microsynth		TTTGGCAGAGGTGGCAAAC
recombinant DNA reagent	Primer Forward: PLIN4	Microsynth		AACCTGCAGGGAAGGTGTTC
recombinant DNA reagent	Primer Forward: PNPLA2	Microsynth		TGGCTTCCCTAACTCAGCTTG
recombinant DNA reagent	Primer Forward: PNPLA3	Microsynth		TGTCAAGGAAAACAGAAGGAAGC
recombinant DNA reagent	Primer Reverse: ACSL3	Microsynth		TGAAAGGTTGCCTTCCTGAG

recombinant DNA reagent	Primer Reverse: ACSL4	Microsynth		TCGCCTCAAGTTGTTGCTC
recombinant DNA reagent	Primer Reverse: AGPAT2	Microsynth		CTTCAAATGAATGGGGAACTGC
recombinant DNA reagent	Primer Reverse: AGPAT3	Microsynth		GCCCGGTACCTTGTGTGAC
recombinant DNA reagent	Primer Reverse: CTCF	Microsynth		GGTTCTCCCAAGCAGGAGCA
recombinant DNA reagent	Primer Reverse: LPCAT2	Microsynth		TCTATGAACCTCGGTTGCCTTC
recombinant DNA reagent	Primer Reverse: MGLL	Microsynth		CAGCCACGCACTCCTCTC
recombinant DNA reagent	Primer Reverse: PLIN3	Microsynth		GATCCACAGGAAGTTCAAGCTG
recombinant DNA reagent	Primer Reverse: PLIN4	Microsynth		TTCCTCCTTCGCTTGCTTC
recombinant DNA reagent	Primer Reverse: PNPLA2	Microsynth		TCATCTCTGGACCTAGCTGTTGC
recombinant DNA reagent	Primer Reverse: PNPLA3	Microsynth		GCAGCGACTCGAGAGAAAGC
recombinant DNA reagent	Primer set: ACSL3	QIAGEN	Cat #: QT01068333	
recombinant DNA reagent	Primer set: ACTB	QIAGEN	Cat #: QT01136772	
recombinant DNA reagent	Primer set: AGPAT2	QIAGEN	Cat #: QT00104888	
recombinant DNA reagent	Primer set: AGPAT3	QIAGEN	Cat #: QT00131481	

recombinant DNA reagent	Primer set: DDIT3	QIAGEN	Cat #: QT01749748	
recombinant DNA reagent	Primer set: DGAT2	QIAGEN	Cat #: QT00134477	
recombinant DNA reagent	Primer set: HMGCR	QIAGEN	Cat #: QT00004081	
recombinant DNA reagent	Primer set: LDLR	QIAGEN	Cat #: QT00045864	
recombinant DNA reagent	Primer set: MGLL	QIAGEN	Cat #: QT01163428	
recombinant DNA reagent	Primer set: PLIN4	QIAGEN	Cat #; QT00112301	
recombinant DNA reagent	Primer set: PNPLA2	QIAGEN	Cat #: QT00111846	
recombinant DNA reagent	Primer set: SOAT1	QIAGEN	Cat #: QT01046472	
recombinant DNA reagent	Primer set: SREBPF1	QIAGEN	Cat #: QT00167055	
recombinant DNA reagent	Primer set: SREBPF1	QIAGEN	Cat #: QT00036897	
recombinant DNA reagent	Primer set: SREBPF2	QIAGEN	Cat #: QT00255204	
recombinant DNA reagent	Primer set: SREBPF2	QIAGEN	Cat #: QT00052052	
recombinant DNA reagent	Primer set: TFAP2A	QIAGEN	Cat #: QT00085225	
recombinant DNA reagent	Primer set: TFAP2C	QIAGEN	Cat #: QT00073073	

sequence-based reagent	siRNA DDIT3	Dharmacon	Cat #: J-062068	
sequence-based reagent	siRNA TFAP2A	Dharmacon	Cat #: J-062799	
sequence-based reagent	siRNA TFAP2C	Dharmacon	Cat #: J-048594	
sequence-based reagent	siRNA APC	QIAGEN	Cat #: S102757251	
sequence-based reagent	siRNA DGAT1	QIAGEN	Cat #: S100978278	
sequence-based reagent	siRNA DGAT2	QIAGEN	Cat #: S100978278	
sequence-based reagent	siRNA GSK3B	QIAGEN	Cat #: S100300335	
sequence-based reagent	siRNA SOAT1	QIAGEN	Cat #: S101428924	
commercial assay or kit	Bio-Rad Protein Assay Kit	Bio-Rad Laboratories	Cat #: 500-0006	
commercial assay or kit	SsoAdvanced SYBR Green Supermix	Bio-Rad Laboratories	Cat #: 1725270	
commercial assay or kit	Triglyceride Colorimetric Assay Kit	Cayman Chemicals	Cat #: 10010303	
commercial assay or kit	Wizard SV gel and PCR Clean-up system	Promega	Cat #: A9281	
commercial assay or kit	RNeasy Mini Kit	QIAGEN	Cat #: 74104	
commercial assay or kit	RNeasy Mini Kit	QIAGEN	Cat #: 74104	
commercial assay or kit	Amplex Red Cholesterol Assay Kit	ThermoFisher Scientific	Cat #: A12216	

commercial assay or kit	SuperScript VILO cDNA Synthesis Kit	ThermoFisher Scientific	Cat #: 11754050	
chemical compound, drug	Wnt Pathway Library	Enzo Life Sciences	Cat #: BML-2838	
chemical compound, drug	BODIPY 493/503	ThermoFisher Scientific	Cat #: D3922	
chemical compound, drug	Hoechst 33342	ThermoFisher Scientific	Cat #: H3570	
chemical compound, drug	Lipofectamine 3000	ThermoFisher Scientific	Cat #: L3000015	
chemical compound, drug	Lipofectamine LTX	ThermoFisher Scientific	Cat #: A12621	
chemical compound, drug	Lipofectamine RNAiMax	ThermoFisher Scientific	Cat #: 13778100	
chemical compound, drug	A-922500	Tocris Bioscience	Cat #: 3587	PMID:18183944
chemical compound, drug	PF-429242	Tocris Bioscience	Cat #: 3354	PMID:17583500
chemical compound, drug	Torin-2	Tocris Bioscience	Cat #: 4248	PMID:21322566

Cells, media, reagents and antibodies

HeLa-MZ cells, a line of HeLa cells selected to be amiable to imaging, were provided by Prof. Lucas Pelkmans (University of Zurich). HeLa cells are not on the list of commonly misidentified cell lines maintained by the International Cell Line Authentication Committee. Our HeLa-MZ cells were authenticated by Microsynth (Balgach, Switzerland), which revealed 100% identity to the DNA profile of the cell line HeLa (ATCC: CCL-2) and 100% identity over all 15 autosomal STRs to the Microsynth's reference DNA profile of HeLa. L

cells (ATCC: CRL-2648) and L Wnt3A cells (ATCC: CRL-2647) were generously provided by Prof. Gisou van der Goot (École Polytechnique Fédérale de Lausanne; EPFL) and cultured as per ATCC recommendations. Cells are mycoplasma negative as tested by GATC Biotech (Konstanz, Germany). Wnt3A-conditioned, and control-conditioned media was prepared from these cells by pooling two subsequent collections of 24h each from confluent cells. Reagents were sourced as follows: Hoechst 33342 and BODIPY 493/503 from Molecular Probes (Eugene, OR); The DGAT1 inhibitor A-922500 and the Membrane Bound Transcription Factor Peptidase, Site 1 (S1P/SREBF) inhibitor PF-429242, and the mTOR inhibitor Torin-2 were from Tocris Bioscience (Zug, Switzerland); lipoprotein-depleted serum (LPDS) was prepared as previously described (Havel et al., 1955); anti-DDIT3 antibodies were from Cell Signaling (L63F7; Leiden, The Netherlands); anti-TFAP2A antibodies were from Abcam (ab52222; Cambridge, UK); fluorescently labeled secondary antibodies from Jackson ImmunoResearch Laboratories (West Grove, PA); 96-well Falcon imaging plates (#353219) were from Corning (Corning, NY); oligonucleotides and small interfering RNA (siRNA) from Dharmacon (SmartPool; Lafayette, CO) or QIAGEN (Venlo, The Netherlands) and the siRNAs used in this work were: GSK3B (S100300335) ; DGAT1 (S100978278); DGAT2 (S100978278); SOAT1 (S101428924); TFAP2A (J-062799); TFAP2C (J-048594); DDIT3 (J-062068); APC (S102757251).

Other chemicals and reagents were obtained from Sigma-Aldrich (St. Louis, MO). Transfections of cDNA and siRNAs were performed using Lipofectamine LTX and Lipofectamine RNAiMax (Invitrogen; Basel, Switzerland) respectively using the supplier's instructions.

Plasmids encoding GSK3B and GSK3B^{S9A}, and were from Addgene (Cambridge, MA) and the SREBF truncations from ATCC; TFAP2A, TFAP2B, and DDIT3 coding sequences were obtained from the Gene Expression Core Facility at the EPFL, and TFAP2C from DNASU (Arizona State University) and cloned into appropriate mammalian expression vectors using Gateway Cloning (Thermo Fisher Scientific). Knock-out cell lines of TFAP2A and DDIT3 were obtained by clonal isolation after transfection of a pX330 Cas9 plasmid (Cong et al., 2013) with appropriate guide sequences (see Supplementary Methods).

Lipid Droplet Quantitation

L Cells were seeded (6 000 cells/well) in imaging plates the day before addition of control-conditioned, or Wnt3a-conditioned media for 24h, before fixation with 3% paraformaldehyde for 20 min. Where necessary, cells were treated with siRNAs and Lipofectamine RNAiMax Reagent (Thermo Fisher) per the manufacturer's instructions for 48 hours before seeding into imaging plates. Lipid droplets and nuclei were labelled with 1µg/mL BODIPY 493/503 (Invitrogen; D3922) and 2µg/mL Hoechst 33342 (Invitrogen; H3570) for 30 min, wash with PBS, and the plate sealed and imaged with ImageXpress Micro XLS (Molecular Devices, Sunnyvale, CA) automated microscope using a 60X air objective. Images were segmented using CellProfiler (Carpenter et al., 2006) to identify and quantify nuclei, cells, and lipid droplets.

Wnt Ligand Screen

L Cells cells were seeded into image plates (6 000 cells/well) the morning before transfection with Lipofectamine 3000 (Invitrogen) as per the manufacturer's instructions with a subset of untagged Wnts from the open source Wnt Project plasmid library (Najdi et al., 2012). Cells were fixed with 3% PFA after 48h, and lipid droplets quantified as above. Data were

normalized to the number of lipid droplets in the empty vector condition. The circular phylogenetic tree was constructed using human Wnt sequences and the Lasergene (v12.1; DNAStar, Madison WI) bioinformatics software.

Wnt Compound Screen

L Cells were seeded into imaging plates (6 000 cells/well) the day before addition of the Wnt Pathway Library (BML-2838； Enzo Life Sciences, Farmingdale, NY) at either 1µM or 10µM, with either control-conditioned or Wnt3a-conditioned media for 24h, before fixation and lipid droplet quantitation as above. Data were normalized by z-score and the average of quadruplicates.

mRNA Determination

Total-RNA extraction was performed using RNeasy Mini Kit from Qiagen (74104) from L Cells or HeLa-MZ according to manufacturer's recommendation. cDNA synthesis was carried out using SuperScript™ VILO™ cDNA Synthesis Kit (Life Technologies AG; Basel, Switzerland) from 250 ng of total RNA. mRNA expression was evaluated using SsoAdvanced SYBR Green Supermix (Bio-Rad Laboratories, Hercules, CA) with 10 ng of cDNA with specific primers of interest on a CFX Connect real-time PCR Detection System(Bio-Rad). Relative amounts of mRNA were calculated by comparative CT analysis with 18S ribosomal RNA used as internal control. All primers are QuantiTect primer from Qiagen (Hilden, Germany) and were: SOAT1 (QT01046472), DGAT2 (QT00134477), ACSL3 (QT01068333), AGPAT2 (QT00104888), AGPAT3 (QT00131481), MGLL (QT01163428), PLIN4 (QT00112301), PNPLA2 (QT00111846), SREBPF1 (QT00167055), SREBPF1 (QT00036897), SREBPF2 (QT00255204), SREBPF2 (QT00052052), DDIT3

(QT01749748), TFAP2A (QT00085225), TFAP2C (QT00073073), ACTB (QT01136772), LDLR (QT00045864), HMGCR (QT00004081).

Lipid Determinations

Cholesterol esters and triglycerides amounts were determined using the Amplex Red Cholesterol Assay Kit (A12216; Thermo Fisher Scientific) and the Triglyceride Colorimetric Assay Kit (10010303; Cayman Chemicals) respectively. Briefly, cells were cultured as needed and scraped directly into lysis buffer (150 mM NaCl, 20 mM HEPES pH 7.4, 1% Triton X-100). Protein concentrations were determined for normalization using Bio-Rad Protein Assay Kit (500-0006) and lipid determinations were made as per the manufacturer's instructions. Cholesterol determinations were made twice, with and without cholesterol esterase, in order to infer the amount of cholesteryl esters.

RNAseq

HeLa-MZ cells were treated in triplicate with control-conditioned, or Wnt3a-conditioned media for 2h or 6h before cells were collected and RNA isolated. Purification of total RNA was done with the RNeasy Mini Kit from Qiagen according to the manufacturer's instructions. The concentration, purity, and integrity of the RNA were measured with the Picodrop Microliter UV-Vis Spectrophotometer (Picodrop), and the Agilent 2100 Bioanalyzer (Agilent Technologies), together with the RNA 6000 Series II Nano Kit (Agilent) according to the manufacturer's instructions. Purified RNAs were sequenced with a HiSeq 4000 (Illumina) at the iGE3 Genomics Platform of the University of Geneva (https://ige3.genomics.unige.ch).

Sequencing reads were mapped to the hg38 genome using bowtie2 in local alignment mode. Then reads were attributed to known exons as defined by the ensembl annotation, and transcript-level read counts were inferred as described in (David et al., 2014). Differential expression was then evaluated by LIMMA (Law et al., 2014) using the log of rpkm values. The fold induction was determined as a ratio of mRNA amounts of Wnt3a to control. Genes with message levels increase more than 1.5-fold, or decreased less than 0.8-fold were collected and tested for pathway enrichment using DAVID bioinformatics resources (v6.8) (Huang da et al., 2009) and the resulting data compiled and plotted using Cytoscape (Shannon et al., 2003) and previously described Matlab scripts (Mercer et al., 2012).

Wnt siRNA Screen Analysis

Data from the genome-wide siRNA screen (Scott et al., 2015) was used to produce the subset of annotated transcription factors (GO:0003700) cellular cholesterol levels after gene silencing provided by AmiGO 2 (version 2.4.26) (Carbon et al., 2009). Data were filtered for genes that increased or decreased total cellular cholesterol a z-score of 1.5 or greater.

Transcription Factor Enrichment

Transcript data from cells treated with Wnt3a (E-MTAB-2872 (Scott et al., 2015)), or fatty acids (GSE21023 (Lockridge et al., 2008), GSE22693 (Xu et al., 2015), GSE42220 (Shaw et al., 2013)) were collected and mRNAs that significantly changed in response to treatment were compiled and analyzed for transcription factor enrichment using GeneGo (MetaCore) bioinformatics software (Thomson Reuters). Data from both conditions was compared and ordered by a sum of ranking.

Promotor Analysis

Promotor sequences from the current (GRCh38) human genome were collected using Regulatory Sequence Analysis Tools (RSAT) software (Medina-Rivera et al., 2015) to collect the non-overlapping upstream promotor sequences (<3 000 bp) of genes of interest which were tested for enriched sequences using either the RSAT's oligo-analysis or Analysis of Motif Enrichment (AME) module of MEME Suite (v.4.12.0) (McLeay and Bailey, 2010). Genes with no non-overlapping upstream region were discarded from the analysis. Identification and quantitation of consensus binding sites was done with either RSAT's matrix-scan or MEME Suite's Motif Alignment and Search Tool (MAST) module using a cut-off of <0.0001 to define a consensus site. Consensus sites from JASPAR (Mathelier et al., 2016) were: DDIT3:CEBPA (MA0019.1), TFAP2A (MA0003.2, MA0810.1), TFAP2C (MA0524.1, MA0524.2).

ChIP-qPCR

Hela-MZ cells were transfected as above with empty vector or pcDna6.2-V5-TFAP2A. After 24h Hela medium was replaced with either: fresh medium (mock), control or Wnt3a-conditional medium. At 48h from transfection cell were incubated with PFA 1% for 8 minutes; after quenching the reaction with glycine 0.125M, cells were resuspended sequentially in the following lysis buffers: lysis buffer I (50mM Hepes-KOH, 140mM NaCl, 1mM EDTA, 10% glycerol, 0.5% of NP-40, 0.25% Triton X-100; adjust final pH to 7.5), lysis buffer II (10mM Tris-HCl pH: 8.0, 200mM NaCl, 1mM EDTA, 0.5mM EGTA; adjust final pH to 8.0), lysis buffer III (10mM Tris-HCl pH: 8.0, 100mM NaCl, 1mM EDTA, 0.5mM EGTA, 0.1% Na-deoxycholate, 0.5% N-lauroylsarcosine; adjust final pH to 8.0) all containing protease inhibitors. Chromatin is sonicated using a Bioruptor Sonicator (Diagenode Inc.) to generate 200- to 1000-bp DNA fragments (30 pulses of 30 s at high

power- total time of 30 min, 30 s ON, 30 s OFF). After microcentrifugation, the supernatant is diluted in buffer III in order to have 2mg of protein in 1ml (1:10 of each sample has been removed and use as input for the relative sample). Chromatin was incubated with 5 µg of antibody (V5 Tag Monoclonal Antibody; R960-25 Thermo Fisher Scientific) on a rotator for 14–16 h at 4°C and 4h hours more after adding 50 µl of magnetic beads (Dynabeads™ Protein G fron Invitrogen). After the reverse cross-linking and elution immunoprecipitated chromatin was purified by columns (Promega Wizard® SV gel and PCR Clean-up system; A9281). Quantitative PCR was performed using the SsoAdvanced SYBR Green Supermix, and an CFX Connect real-time PCR Detection System (Bio-Rad Laboratories, Hercules, CA) according to manufacturer's instructions. Primers used are listed below. Dissociation curves after amplification showed that all primer pairs generated single products. The amount of PCR product amplified was calculated as percent of the input. A genomic region of an intron in Myc gene (CTCF, CCCTC-Binding Factor) was used as negative control.

List of Primers for ChIP-qPCR

MGLL

Forward: GAACCCAGCTCAGTTCAGG

Reverse: CAGCCACGCACTCCTCTC

PLIN4

Forward: AACCTGCAGGGAAGGTGTTC

Reverse: TTCCTCCTTCGCTTGCTTC

ACSL3

Forward: TGAGCTCTCTTTGCTTGGTG

Reverse: TGAAAGGTTGCCTTCCTGAG

AGPAT3

Forward: ACCCAAGCTCAGCAAGTCC

Reverse: GCCCGGTACCTTGTGTGAC

ACSL4

Forward: AAGGACATCCCGAAACACAC

Reverse: TCGCCTCAAGTTGTTGCTC

AGPAT2

Forward: GGCCTAAGGCAAAAGGATGTG

Reverse: CTTCAAATGAATGGGGAACTGC

PNPLA3

Forward: TGTCAAGGAAAACAGAAGGAAGC

Reverse: GCAGCGACTCGAGAGAAAGC

PNPLA2

Forward: TGGCTTCCCTAACTCAGCTTG

Reverse: TCATCTCTGGACCTAGCTGTTGC

LPCAT2

Forward: AGGGGAAGTGGTTGCTCAATG

Reverse: TCTATGAACCTCGGTTGCCTTC

PLIN3

Forward: TTTGGCAGAGGTGGCAAAC

Reverse: GATCCACAGGAAGTTCAAGCTG

CTCF site inside the gene Myc:

Foward: GCCAGTCCAACCGGCTTATG

Reverse: GGTTCTCCCAAGCAGGAGCA

Construction of Gene Edited Knock Out Cell Lines

The guide sequences used to construct specific CRISPR/Cas9 vectors were determined using the CRISPR Design Tool(Ran et al., 2013) and were:

TFAP2A

Fwd: CACCGGAGTAAGGATCTTGCGACT

Rev: AAACAGTCGCAAGATCCTTACTCC

DDIT3

Fwd: CACCGGCACCTATATCTCATCCCC

Rev: AAACGACTGATCCAACTGCAGAGAC

These sequences were used to create insert the target sequence into the pX330 vector using Golden Gate Assembly (New England Biolabs) and transfected into cells as described in the

638 Methods. Knock-out clones were isolated by serial dilution and confirmed by Western
639 blotting and activity assays.
640
641
642

Figure and Table Legend

Figure 1. The Wnt pathway and the regulation of lipid droplets.

A-B. HeLa-MZ cells were transfected with plasmids encoding wild-type or a S9A mutant of GSK3B 24h before the addition of Wnt-3a- or control-conditioned media (CM) for a further 24h. Cells were fixed, labeled with BODIPY (lipid droplets, green) and Hoechst 33342 (nuclei, magenta), and imaged by light microscopy. In **B.** the number of lipid droplets was quantified by automated microscopy (bar graph), and the data are presented as the mean number of lipid droplets per cell of 5 independent experiments ± SEM, normalized to the control condition.

C-D. As in (A), except that HeLa-MZ cells (**C**) or L Cells (**D**) were transfected with siRNAs against the indicated targets for 48h, before the addition of Wnt3a. Efficient silencing was confirmed by qPCR (Fig. 1 - Fig.Sup. 1B) and the data are presented as the mean number of lipid droplets per cell of 3 independent experiments ± SEM, normalized to the control condition.

E. L cells were incubated with the indicated compounds together with Wnt3a for 24h, processed and analyzed as in (A) and the data are presented as the mean number of lipid droplets per cell of 5 independent experiments ± SEM, normalized to the control condition.

F. Evolutionary relationship of the 19 Wnt ligands. Colour indicates ability to induce lipid droplets as detailed in (G).

G. L Cells were transfected with plasmids containing each of Wnt ligand for 48h, imaged and analyzed as in (A). Data are normalized to the empty vector control and were tested for significance and are presented as the mean number of lipid droplets per cell of 2 independent replicates of the screen ± SEM, normalized to the control condition. The data are color-coded from a high (light) to a low (dark) number of lipid droplets induced by each Wnt ligand.

H-I. High content image-based screen of a library of compounds that affect the Wnt pathway in HeLa-MZ cells. Cells were incubated for 24h with Wnt-3a- or control-conditioned media for 24h in the presence of the compounds at 1µM and 10µM, fixed, labeled with BODIPY (lipid droplets) and Hoechst 33342 (nuclei) and imaged by automated microscopy. The number of droplets per cell was counted and the zscores established, in order to quantify the ability of each compounds to induce lipid droplets in untreated cells (H, left panel), or to inhibit lipid droplet formation in Wnt3a-treated cells (H, right panel). Panel I illustrates the effects of compounds that induce droplet formation (left column) or that do (Trichostatin A) or do not (niclosamide, hexachlorophene) inhibit droplet formation (right column) in Wnt3a-treated cells. Nuclei are in magenta, and lipid droplets in green.

Green bars, control-conditioned media (control CM); Red bars, Wnt3a-conditioned media (Wnt3a CM). In this figure, pValues are indicate as: *, <0.05; **, <0.005, and n.s., not significant.

Figure 2. mRNA profiling and analysis of gene expression of cells treated with Wnt3a.

A-B. HeLa-MZ cells were treated with control- or Wnt3a-conditioned media for 2h or 6h before RNA isolation and RNAseq analysis. Panel (A) shows the pathway enrichment of perturbed mRNAs. Node size indicates number of genes in each ontology and colour the statistical strength of the enrichment. Edge thickness indicates the strength of overlap of related ontologies. From (A), the fold change of transcription factors amounts in response to Wnt3a is shown in panel B.

C. The ability of TFAP2 family member TFAP2A to bind to regulatory regions of lipid droplet at lipid metabolic enzyme genes was tested by ChIP-qPCR (see Methods). Data are presented as the mean DNA amounts normalized to the negative control (CTCF) of 3

691 independent experiments ± SEM. (*) indicates a p-value <0.05; (**) indicates a p-value
692 <0.005. Inset; re-scaled view of signal of the control conditions.
693
694 **Figure 3. The TFAP2 family of transcription factors are both necessary and sufficient to**
695 **mediated lipid droplet accumulation.**
696 **A-B.** L Cells were treated with siRNAs against the indicated targets for 48h before the
697 addition of Wnt3a-conditioned medium for an additional 24h. Cells were then fixed, labeled,
698 imaged and analyzed by automated microscopy as in Fig 1A. In (A), data are presented as the
699 normalized mean number of lipid droplets per cell of 5 independent experiments ± SEM.
700 Cells treated with non-target siRNAs or with siRNAs to both TFAP2A and TFAB2C are
701 shown in panel B (nuclei in magenta; lipid droplets in green).
702 **C.** L cells were treated with siRNAs against both TFAP2A and TFAP2C or with non-
703 targeting controls as in (A), before the addition of Wnt3a- or control-conditioned media for
704 an additional 24h. RNA was isolated and analyzed by qPCR using primers to the indicated
705 genes, and that data are expressed relative to the non-target control and are presented as the
706 mean mRNA amounts of 2-5 independent experiments ± SEM.
707 **D-E.** HeLa-MZ cells were transfected with targeted CRISPR/Cas9 plasmids against
708 TFAP2A. The corresponding knock-out clones as well as control cells were treated with
709 Wnt3a-conditioned media for 24h. In **D**, the number of lipid droplets was quantified as in Fig
710 1A and is expressed as fold induction relative to the control cells in 5 independent
711 experiments ± SEM. Inset: TFAP2A protein levels of each clone determined by Western blot.
712 Arrow indicate position of 50 kDa marker. Representative images are shown in E (nuclei in
713 magenta; lipid droplets in green).
714 **F-H.** L Cells were transfected or not with mCherry-tagged TFAP2 family members for 48h
715 before fixation, labeling and imaging as in Fig 1A. The mean number of lipid droplets per

cell expressing each mCherry-tagged TFAP2 protein was counted, and is expressed, as in panel (D), as fold induction relative to the control cells in 6 independent experiments ± SEM. Panel G shows cells expressing each mCherry-tagged TFAP2 protein (Blue, nucleus; Green, lipid droplets; Red, TFAP2-mCherry fusion proteins), and panel H shows the number of lipid droplets per cell in cells overexpression TFAP2C-mCherry, binned by their nuclear:cytoplasmic distribution. Data are the mean lipid droplets per cell ± SEM for 450 cells.

I. L Cells were treated as in **F** before extraction and determination of the indicated mRNAs by qPCR. Data are presented as the mean mRNA amounts of 2-5 independent experiments ± SEM.

In this figure, (*) indicates a p-value <0.05.

Figure 4. DDIT3 is both necessary and sufficient to mediated lipid droplet accumulation

A-B. qPCR of DDIT3, DGAT2 and SOAT1 after overexpression of DDIT3-mCherry (A), or siRNAs to DDIT3 (B). Data are presented as the mean of 2-5 independent experiments ± SEM.

C. L cells were treated, processed and analyzed like in Fig 3A, except that they were transfected with siRNAs to DDIT3 before stimulation with Wnt3a. Data are presented as the normalized mean number of lipid droplets per cell of 3 independent experiments ± SEM. (*) indicates a p-value <0.05. Panel E shows cells treated with non-target or anti-DDIT3 siRNAs (magenta, nucleus; green, lipid droplets).

D. HeLa-MZ CRISPR/Cas9 clones were prepared and analysed as in Fig 3D. Data are expressed as fold induction relative to the control cells in 5 independent experiments ± SEM. Inset: DDIT3 protein levels of each clone determined by Western blot. Arrow indicate

position of 25 kDa marker. Representative images are shown (nuclei in magenta; lipid droplets in green).

E. L cells were treated, processed and analyzed like in Fig 3F, except that they were transfected with a plasmid encoding DDIT3-mCherry. Data are presented as the normalized mean number of lipid droplets per cell of 6 independent experiments ± SEM. (*) indicates a p-value <0.05. Panel E shows cells expressing or not DDIT3-mCherry (blue, nucleus; green, lipid droplets, red, DDIT3-mCherry fusion protein).

In this figure, (*) indicates a p-value <0.05.

Figure 1 – Figure Supplement 1. Lipid droplet accumulation in response to Wnt3a: combinatorial treatments against lipid droplet enzymes by RNAi and chemical inhibitors.

A. L cells were treated with the indicated siRNAs for 48h before addition of the indicated compounds together with control, or Wnt3a, conditioned media and incubation for an additional 24h. Cells were then fixed, stained and lipid droplet number quantified as in Fig 1A. Data are presented as the normalized mean number of lipid droplets per cell of 3 independent experiments ± SEM.

B. L Cells were treated as in Fig. 1A with the indicated siRNAs and the amounts of the corresponding mRNA were determined by qPCR.

Figure 2 – Figure Supplement 1. Datamining for putative lipid droplet transcriptional regulators.

A. Transcription factors that influence cellular cholesterol amounts from a genome-wide screen of cholesterol regulatory genes (Scott et al., 2015). Node size is proportional to the

absolute z-score difference from the control, and the colour indicates increased (green) or decreased (blue) cellular cholesterol levels.

B. Existing mRNA profiling experiments of cells treated with Wnt3a (blue), or perturbations likely to induce lipid droplet accumulation (see methods) (pink), were analyzed for enrichment of genes linked to known transcriptions factors to identify candidate transcription factors linking Wnt3a to lipid droplet biogenesis.

Figure 2 – Figure Supplement 2. The consensus binding sites of TFAP2 family members are overrepresented in lipid droplet genes.

A. Enrichment of known transcription factor consensus sequences in lipid droplet genes.

B. TFAP2A and TFAP2C consensus binding site motifs.

C. Distribution of TFAP2 consensus sites in the promotor region of genes annotated to be lipid droplet related.

Figure 2 – Figure Supplement 3. Effect of Wnt3a on DDIT3 protein and mRNA amounts in L Cells.

Cells were treated with control- or Wnt3a-conditioned media for the indicated times before lysis.

A. mRNA was extracted from L Cells cells and amounts were determined by qPCR.

B. Cell extracts were analyzed by SDS-PAGE and Western blot using antibodies against the indicated proteins.

Figure 2 – Figure Supplement 4. SREBF activity does not significantly influence lipid droplet number.

A. L Cells were transfected or not with constitutively-active truncation mutants of SREBF1a, SREBF1c, and SREBF2 for 24h before addition of control- or Wnt3a-conditioned media for an additional 24h. Cells were fixed, labeled and imaged by automated microscopy as in Fig 1A. Data are box-and-whisker plots of a representative experiment.

B. L Cells were treated with the indicated chemical inhibitors simultaneously with the conditioned media, and processed as (A). PF-429242; inhibitor of the SREBF site 1 protease (S1P). Torin-2; mTOR inhibitor.

C. L Cells were transfected as in **A.** before mRNA extraction and quantitation of HMGCR and LDLR mRNAs by qPCR.

Figure 3 – Figure Supplement 1. Characterization of lipid droplets by PLIN1a-GFP, cholesterol esters and triglycerides.

A. L Cells were treated with the indicated siRNAs for 48h before an additional 24h with control-, or Wnt3a-conditioned media before cells were collected and assayed for protein and cholesterol ester content (see methods). Data are the mean normalized increase in triglycerides of two replicates ± SEM.

B. CRISPR clones were treated for 24h with control- or Wnt3a-conditioned media before lysis and determination of protein and triglyceride content (see methods). Data are the mean normalized increase in triglycerides of two replicates ± SEM.

C-D. CRISPR cells were transfected PLIN1a-GFP and treated as in **B.** before fixation, staining and determination of lipid droplet number by automated microscopy (representative images in **C.**). Data are presented in **D.** and are the mean relative induction of lipid droplets with at least 3 000 cells measured per condition and are representative of two independent experiments and the SEM for each condition.

E. HeLa-MZ were transfected with the indicated plasmids (control; LAMP1-mCherry) for 36h before lipid and protein determination as in **A-B.** Data are the mean of two replicates ± SEM.

F-G. HeLa-MZ were co-transfected with the indicated plasmids (control; LAMP1-mCherry) and PLIN1a-GFP for 36h before quantitation as in **C-D.** Data are presented in **G.** and are the mean relative induction of lipid droplets with at least 500 cells measured per condition and are representative of two independent experiments and the SEM for each condition.

Figure 3 – Figure Supplement 2. Characterization of knock-down efficiencies and relative over-expression levels by qPCR.

A-D. mRNA was extracted from HeLa-MZ (**B,D**) or L Cells (**A,C**) transfected with either siRNAs (72h; **A**,**C**) or the indicated plasmids (48h **B**,**D**) and amounts determined by qPCR. Data are the normalized means of 2 or 3 replicates, presented +/- SEM. In this figure, (*) indicates a p-value <0.05.

Figure 4 – Figure Supplement 1. DDIT3 and lipid homeostasis.

A. Location of DDIT3:CEBPA consensus sites in the promotor regions of the transcription factors Fig. 2B reported to be involved in lipid homeostasis. Indicated is the pvalue of the match of the consensus motif.

B. HeLa-MZ cells were treated with siRNAs to the indicated target proteins for 48h, and then further incubated for 24h in the presence of control- or Wnt3a-conditioned media. Cells were then fixed, stained and the number of lipid droplets was quantified as in Fig 1A. Data are presented as the normalized mean number of lipid droplets per cell of 3 independent experiments ± SEM.

C. DDIT3-mCherry was overexpressed in HeLa-MZ cells for 24h and then further incubated for 24h in the presence of control, or Wnt3a, conditioned media. Cells were then fixed and labeled, and the number of lipid droplets per cell expressing DDIT3-mCherry was quantified as in Fig 4F. Data are presented as the normalized mean number of lipid droplets per cell of 5 independent experiments ± SEM.

D. CRISPR clones and the Hela-MZ parental line were transfected with the indicated plasmids for 36h before addition of control-, or Wnt3a-conditioned media for and additional 24h. Cells were fixed, stained and the number of lipid droplets quantified by automated microscopy and transfected cells were identified by the presence of mCherry. Data are expressed as the normalized mean induction of lipid droplets per transfected cell of 3 independent experiments ± SEM.

Acknowledgements

We are grateful to Christian Iseli, Nicolas Guex, and Ioannis Xenarios from Vital-IT and the Swiss Institute of Bioinformatics for indispensable guidance on the interpretation of the transcriptomics data and critical reading of the manuscript. Support was from the Swiss National Science Foundation, the NCCR in Chemical Biology and LipidX from the Swiss SystemsX.ch Initiative, evaluated by the Swiss National Science Foundation (to J. G.). C. C. S. has been supported by fellowships from the Human Frontier Science Program and the Canadian Institutes of Health Research.

Competing Interests

The authors declare no competing interests.

Materials & Correspondence

Correspondence and requests to Jean Gruenberg.

Figure Supplements

Figure 1 – figure supplement 1: Lipid droplet accumulation in response to Wnt3a: combinatorial treatments against lipid droplet enzymes by RNAi and chemical inhibitors.

Figure 2 – figure supplement 1: Datamining for putative lipid droplet transcriptional regulators.

Figure 2 – figure supplement 2: The consensus binding sites of TFAP2 family members are overrepresented in lipid droplet genes.

Figure 2 – figure supplement 3: Effect of Wnt3a on DDIT3 protein and mRNA amounts in L Cells.

Figure 2 – figure supplement 4: SREBF activity does not significantly influence lipid droplet number.

Figure 3 – figure supplement 1: Characterization of lipid droplets by PLIN1a-GFP, cholesterol esters and triglycerides.

Figure 3 – figure supplement 2. Characterization of knock-down efficiencies and relative over-expression levels my qPCR.

Figure 4 – figure supplement 1: DDIT3 and lipid homeostasis.

Figure Source Data

Figure 1 – Source Data 1: Effect of Wnt pathway related compounds on lipid droplet induction.

Figure 2 – Source Data 1: Effect of silencing transcription factors on cellular cholesterol amounts.

888 Figure 2 – Source Data 2: Comparative enrichment of transcriptional targets in cells treated
889 with Wnt3a or fatty acid perturbation.
890 Figure 2 – Source Data 3: TFAP2 family member consensus binding sites in lipid droplet
891 genes.
892

References

ACKERS, I. & MALGOR, R. 2018. Interrelationship of canonical and non-canonical Wnt signalling pathways in chronic metabolic diseases. *Diab Vasc Dis Res,* 15**,** 3-13.

BARISCH, C. & SOLDATI, T. 2017. Breaking fat! How mycobacteria and other intracellular pathogens manipulate host lipid droplets. *Biochimie*.

BARNEDA, D. & CHRISTIAN, M. 2017. Lipid droplet growth: regulation of a dynamic organelle. *Curr Opin Cell Biol,* 47**,** 9-15.

BOZEK, K., RELOGIO, A., KIELBASA, S. M., HEINE, M., DAME, C., KRAMER, A. & HERZEL, H. 2009. Regulation of clock-controlled genes in mammals. *PLoS One,* 4**,** e4882.

CARBON, S., IRELAND, A., MUNGALL, C. J., SHU, S., MARSHALL, B., LEWIS, S., AMI, G. O. H. & WEB PRESENCE WORKING, G. 2009. AmiGO: online access to ontology and annotation data. *Bioinformatics,* 25**,** 288-9.

CARPENTER, A. E., JONES, T. R., LAMPRECHT, M. R., CLARKE, C., KANG, I. H., FRIMAN, O., GUERTIN, D. A., CHANG, J. H., LINDQUIST, R. A., MOFFAT, J., GOLLAND, P. & SABATINI, D. M. 2006. CellProfiler: image analysis software for identifying and quantifying cell phenotypes. *Genome Biol,* 7**,** R100.

CHANG, T. Y., CHANG, C. C., LU, X. & LIN, S. 2001. Catalysis of ACAT may be completed within the plane of the membrane: a working hypothesis. *J Lipid Res,* 42**,** 1933-8.

CHAUHAN, S., GOODWIN, J. G., CHAUHAN, S., MANYAM, G., WANG, J., KAMAT, A. M. & BOYD, D. D. 2013. ZKSCAN3 is a master transcriptional repressor of autophagy. *Mol Cell,* 50**,** 16-28.

914 CHIKKA, M. R., MCCABE, D. D., TYRA, H. M. & RUTKOWSKI, D. T. 2013. C/EBP homologous
915 protein (CHOP) contributes to suppression of metabolic genes during endoplasmic
916 reticulum stress in the liver. *J Biol Chem,* 288**,** 4405-15.
917 CONG, L., RAN, F. A., COX, D., LIN, S., BARRETTO, R., HABIB, N., HSU, P. D., WU, X., JIANG,
918 W., MARRAFFINI, L. A. & ZHANG, F. 2013. Multiplex genome engineering using
919 CRISPR/Cas systems. *Science,* 339**,** 819-23.
920 DAI, C., STOLZ, D. B., KISS, L. P., MONGA, S. P., HOLZMAN, L. B. & LIU, Y. 2009. Wnt/beta-
921 catenin signaling promotes podocyte dysfunction and albuminuria. *J Am Soc*
922 *Nephrol,* 20**,** 1997-2008.
923 DAVID, F. P., DELAFONTAINE, J., CARAT, S., ROSS, F. J., LEFEBVRE, G., JAROSZ, Y., SINCLAIR,
924 L., NOORDERMEER, D., ROUGEMONT, J. & LELEU, M. 2014. HTSstation: a web
925 application and open-access libraries for high-throughput sequencing data analysis.
926 *PLoS One,* 9**,** e85879.
927 ECKERT, D., BUHL, S., WEBER, S., JAGER, R. & SCHORLE, H. 2005. The AP-2 family of
928 transcription factors. *Genome Biol,* 6**,** 246.
929 FRIEDMAN, J. R. & KAESTNER, K. H. 2006. The Foxa family of transcription factors in
930 development and metabolism. *Cell Mol Life Sci,* 63**,** 2317-28.
931 HAVEL, R. J., EDER, H. A. & BRAGDON, J. H. 1955. The distribution and chemical composition
932 of ultracentrifugally separated lipoproteins in human serum. *J Clin Invest,* 34**,** 1345-
933 53.
934 HAWKINS, J. L., ROBBINS, M. D., WARREN, L. C., XIA, D., PETRAS, S. F., VALENTINE, J. J.,
935 VARGHESE, A. H., WANG, I. K., SUBASHI, T. A., SHELLY, L. D., HAY, B. A., LANDSCHULZ,
936 K. T., GEOGHEGAN, K. F. & HARWOOD, H. J., JR. 2008. Pharmacologic inhibition of
937 site 1 protease activity inhibits sterol regulatory element-binding protein processing

and reduces lipogenic enzyme gene expression and lipid synthesis in cultured cells and experimental animals. *J Pharmacol Exp Ther,* 326**,** 801-8.

HOLL, D., KUCKENBERG, P., WOYNECKI, T., EGERT, A., BECKER, A., HUSS, S., STABENOW, D., ZIMMER, A., KNOLLE, P., TOLBA, R., FISCHER, H. P. & SCHORLE, H. 2011. Transgenic overexpression of Tcfap2c/AP-2gamma results in liver failure and intestinal dysplasia. *PLoS One,* 6**,** e22034.

HUANG DA, W., SHERMAN, B. T. & LEMPICKI, R. A. 2009. Systematic and integrative analysis of large gene lists using DAVID bioinformatics resources. *Nat Protoc,* 4**,** 44-57.

JORNAYVAZ, F. R. & SHULMAN, G. I. 2010. Regulation of mitochondrial biogenesis. *Essays Biochem,* 47**,** 69-84.

KANG, Y. A., SANALKUMAR, R., O'GEEN, H., LINNEMANN, A. K., CHANG, C. J., BOUHASSIRA, E. E., FARNHAM, P. J., KELES, S. & BRESNICK, E. H. 2012. Autophagy driven by a master regulator of hematopoiesis. *Mol Cell Biol,* 32**,** 226-39.

KIM, N. G., XU, C. & GUMBINER, B. M. 2009. Identification of targets of the Wnt pathway destruction complex in addition to beta-catenin. *Proc Natl Acad Sci U S A,* 106**,** 5165-70.

KONIGE, M., WANG, H. & SZTALRYD, C. 2014. Role of adipose specific lipid droplet proteins in maintaining whole body energy homeostasis. *Biochim Biophys Acta,* 1842**,** 393-401.

LAW, C. W., CHEN, Y., SHI, W. & SMYTH, G. K. 2014. voom: Precision weights unlock linear model analysis tools for RNA-seq read counts. *Genome Biol,* 15**,** R29.

LI, D., ZHANG, Y., XU, L., ZHOU, L., WANG, Y., XUE, B., WEN, Z., LI, P. & SANG, J. 2010. Regulation of gene expression by FSP27 in white and brown adipose tissue. *BMC Genomics,* 11**,** 446.

LI, Q. & DASHWOOD, R. H. 2004. Activator protein 2alpha associates with adenomatous polyposis coli/beta-catenin and Inhibits beta-catenin/T-cell factor transcriptional activity in colorectal cancer cells. *J Biol Chem,* 279**,** 45669-75.

LI, Q., LOHR, C. V. & DASHWOOD, R. H. 2009. Activator protein 2alpha suppresses intestinal tumorigenesis in the Apc(min) mouse. *Cancer Lett,* 283**,** 36-42.

LI, X., WANG, W., WANG, J., MALOVANNAYA, A., XI, Y., LI, W., GUERRA, R., HAWKE, D. H., QIN, J. & CHEN, J. 2015. Proteomic analyses reveal distinct chromatin-associated and soluble transcription factor complexes. *Mol Syst Biol,* 11**,** 775.

LIU, J., WU, X., MITCHELL, B., KINTNER, C., DING, S. & SCHULTZ, P. G. 2005. A small-molecule agonist of the Wnt signaling pathway. *Angew Chem Int Ed Engl,* 44**,** 1987-90.

LOCKRIDGE, J. B., SAILORS, M. L., DURGAN, D. J., EGBEJIMI, O., JEONG, W. J., BRAY, M. S., STANLEY, W. C. & YOUNG, M. E. 2008. Bioinformatic profiling of the transcriptional response of adult rat cardiomyocytes to distinct fatty acids. *J Lipid Res,* 49**,** 1395-408.

LU, W., LIN, C., ROBERTS, M. J., WAUD, W. R., PIAZZA, G. A. & LI, Y. 2011. Niclosamide suppresses cancer cell growth by inducing Wnt co-receptor LRP6 degradation and inhibiting the Wnt/beta-catenin pathway. *PLoS One,* 6**,** e29290.

MARTIN, S. & PARTON, R. G. 2006. Lipid droplets: a unified view of a dynamic organelle. *Nat Rev Mol Cell Biol,* 7**,** 373-8.

MATHELIER, A., FORNES, O., ARENILLAS, D. J., CHEN, C. Y., DENAY, G., LEE, J., SHI, W., SHYR, C., TAN, G., WORSLEY-HUNT, R., ZHANG, A. W., PARCY, F., LENHARD, B., SANDELIN, A. & WASSERMAN, W. W. 2016. JASPAR 2016: a major expansion and update of the open-access database of transcription factor binding profiles. *Nucleic Acids Res,* 44**,** D110-5.

MATSU-URA, T., DOVZHENOK, A., AIHARA, E., ROOD, J., LE, H., REN, Y., ROSSELOT, A. E., ZHANG, T., LEE, C., OBRIETAN, K., MONTROSE, M. H., LIM, S., MOORE, S. R. & HONG, C. I. 2016. Intercellular Coupling of the Cell Cycle and Circadian Clock in Adult Stem Cell Culture. *Mol Cell,* 64**,** 900-912.

MCLEAY, R. C. & BAILEY, T. L. 2010. Motif Enrichment Analysis: a unified framework and an evaluation on ChIP data. *BMC Bioinformatics,* 11**,** 165.

MEDINA-RIVERA, A., DEFRANCE, M., SAND, O., HERRMANN, C., CASTRO-MONDRAGON, J. A., DELERCE, J., JAEGER, S., BLANCHET, C., VINCENS, P., CARON, C., STAINES, D. M., CONTRERAS-MOREIRA, B., ARTUFEL, M., CHARBONNIER-KHAMVONGSA, L., HERNANDEZ, C., THIEFFRY, D., THOMAS-CHOLLIER, M. & VAN HELDEN, J. 2015. RSAT 2015: Regulatory Sequence Analysis Tools. *Nucleic Acids Res,* 43**,** W50-6.

MELO, R. C. & WELLER, P. F. 2016. Lipid droplets in leukocytes: Organelles linked to inflammatory responses. *Exp Cell Res,* 340**,** 193-7.

MERCER, J., SNIJDER, B., SACHER, R., BURKARD, C., BLECK, C. K., STAHLBERG, H., PELKMANS, L. & HELENIUS, A. 2012. RNAi screening reveals proteasome- and Cullin3-dependent stages in vaccinia virus infection. *Cell Rep,* 2**,** 1036-47.

MEYERS, A., WEISKITTEL, T. M. & DALHAIMER, P. 2017. Lipid Droplets: Formation to Breakdown. *Lipids,* 52**,** 465-475.

NAJDI, R., PROFFITT, K., SPROWL, S., KAUR, S., YU, J., COVEY, T. M., VIRSHUP, D. M. & WATERMAN, M. L. 2012. A uniform human Wnt expression library reveals a shared secretory pathway and unique signaling activities. *Differentiation,* 84**,** 203-13.

PARK, S., GWAK, J., CHO, M., SONG, T., WON, J., KIM, D. E., SHIN, J. G. & OH, S. 2006. Hexachlorophene inhibits Wnt/beta-catenin pathway by promoting Siah-mediated beta-catenin degradation. *Mol Pharmacol,* 70**,** 960-6.

1009 PRESTWICH, T. C. & MACDOUGALD, O. A. 2007. Wnt/beta-catenin signaling in adipogenesis
1010 and metabolism. *Curr Opin Cell Biol,* 19**,** 612-7.
1011 RAN, F. A., HSU, P. D., WRIGHT, J., AGARWALA, V., SCOTT, D. A. & ZHANG, F. 2013. Genome
1012 engineering using the CRISPR-Cas9 system. *Nat Protoc,* 8**,** 2281-2308.
1013 ROMMELAERE, S., MILLET, V., VU MANH, T. P., GENSOLLEN, T., ANDREOLETTI, P.,
1014 CHERKAOUI-MALKI, M., BOURGES, C., ESCALIERE, B., DU, X., XIA, Y., IMBERT, J.,
1015 BEUTLER, B., KANAI, Y., MALISSEN, B., MALISSEN, M., TAILLEUX, A., STAELS, B.,
1016 GALLAND, F. & NAQUET, P. 2014. Sox17 regulates liver lipid metabolism and
1017 adaptation to fasting. *PLoS One,* 9**,** e104925.
1018 SARDIELLO, M., PALMIERI, M., DI RONZA, A., MEDINA, D. L., VALENZA, M., GENNARINO, V.
1019 A., DI MALTA, C., DONAUDY, F., EMBRIONE, V., POLISHCHUK, R. S., BANFI, S.,
1020 PARENTI, G., CATTANEO, E. & BALLABIO, A. 2009. A gene network regulating
1021 lysosomal biogenesis and function. *Science,* 325**,** 473-7.
1022 SCOTT, C. C., VOSSIO, S., VACCA, F., SNIJDER, B., LARIOS, J., SCHAAD, O., GUEX, N.,
1023 KUZNETSOV, D., MARTIN, O., CHAMBON, M., TURCATTI, G., PELKMANS, L. &
1024 GRUENBERG, J. 2015. Wnt directs the endosomal flux of LDL-derived cholesterol and
1025 lipid droplet homeostasis. *EMBO Rep,* 16**,** 741-52.
1026 SETHI, J. K. & VIDAL-PUIG, A. 2010. Wnt signalling and the control of cellular metabolism.
1027 *Biochem J,* 427**,** 1-17.
1028 SHANNON, P., MARKIEL, A., OZIER, O., BALIGA, N. S., WANG, J. T., RAMAGE, D., AMIN, N.,
1029 SCHWIKOWSKI, B. & IDEKER, T. 2003. Cytoscape: a software environment for
1030 integrated models of biomolecular interaction networks. *Genome Res,* 13**,** 2498-504.
1031 SHAW, B., LAMBERT, S., WONG, M. H., RALSTON, J. C., STRYJECKI, C. & MUTCH, D. M. 2013.
1032 Individual saturated and monounsaturated fatty acids trigger distinct transcriptional

networks in differentiated 3T3-L1 preadipocytes. *J Nutrigenet Nutrigenomics,* 6**,** 1-15.

SHIMANO, H., HORTON, J. D., SHIMOMURA, I., HAMMER, R. E., BROWN, M. S. & GOLDSTEIN, J. L. 1997. Isoform 1c of sterol regulatory element binding protein is less active than isoform 1a in livers of transgenic mice and in cultured cells. *J Clin Invest,* 99**,** 846-54.

SOLT, L. A., WANG, Y., BANERJEE, S., HUGHES, T., KOJETIN, D. J., LUNDASEN, T., SHIN, Y., LIU, J., CAMERON, M. D., NOEL, R., YOO, S. H., TAKAHASHI, J. S., BUTLER, A. A., KAMENECKA, T. M. & BURRIS, T. P. 2012. Regulation of circadian behaviour and metabolism by synthetic REV-ERB agonists. *Nature,* 485**,** 62-8.

STAMBOLIC, V. & WOODGETT, J. R. 1994. Mitogen inactivation of glycogen synthase kinase-3 beta in intact cells via serine 9 phosphorylation. *Biochem J,* 303 (Pt 3)**,** 701-4.

THIAM, A. R. & BELLER, M. 2017. The why, when and how of lipid droplet diversity. *J Cell Sci,* 130**,** 315-324.

UBEDA, M., WANG, X. Z., ZINSZNER, H., WU, I., HABENER, J. F. & RON, D. 1996. Stress-induced binding of the transcriptional factor CHOP to a novel DNA control element. *Mol Cell Biol,* 16**,** 1479-89.

UCHIYAMA, Y. & ASARI, A. 1984. A morphometric study of the variations in subcellular structures of rat hepatocytes during 24 hours. *Cell Tissue Res,* 236**,** 305-15.

VIBHAKAR, R., FOLTZ, G., YOON, J. G., FIELD, L., LEE, H., RYU, G. Y., PIERSON, J., DAVIDSON, B. & MADAN, A. 2007. Dickkopf-1 is an epigenetically silenced candidate tumor suppressor gene in medulloblastoma. *Neuro Oncol,* 9**,** 135-44.

XU, L., XIA, X., ARSHAD, M. & ZHOU, L. 2015. Gene expression profile in the fat tissue of Fsp27 deficient mice. *Genom Data,* 5**,** 326-8.

ZHANG, M., MAHONEY, E., ZUO, T., MANCHANDA, P. K., DAVULURI, R. V. & KIRSCHNER, L. S. 2014. Protein kinase A activation enhances beta-catenin transcriptional activity through nuclear localization to PML bodies. *PLoS One,* 9**,** e109523.

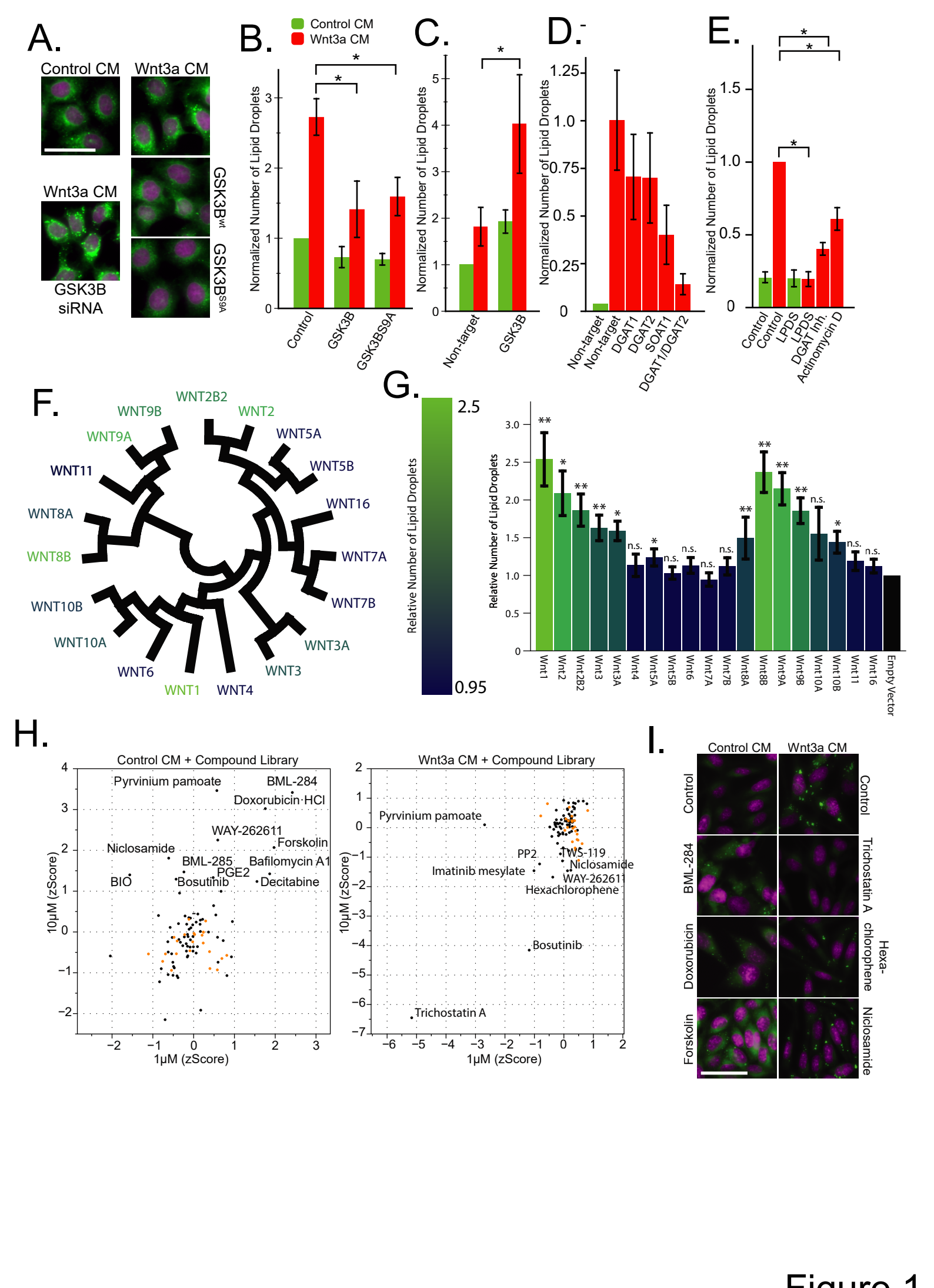
A.
Control CM
Wnt3a CM
Wnt3a CM
GSK3B siRNA
GSK3B^wt
GSK3B^S9A
B.
Control CM
Wnt3a CM
Normalized Number of Lipid Droplets
Control
GSK3B
GSK3BS9A
C.
Normalized Number of Lipid Droplets
Non-target
GSK3B
D.
Normalized Number of Lipid Droplets
Non-target
Non-target
DGAT1
DGAT2
SOAT1
DGAT1/DGAT2
E.
Normalized Number of Lipid Droplets
Control
Control
LPDS
LPDS
DGAT Inh.
Actinomycin D
F.
WNT2B2
WNT9B
WNT2
WNT9A
WNT5A
WNT11
WNT5B
WNT16
WNT8A
WNT7A
WNT8B
WNT7B
WNT10B
WNT3A
WNT10A
WNT6
WNT3
WNT1
WNT4
G.
Relative Number of Lipid Droplets
2.5
0.95
Relative Number of Lipid Droplets
Wnt1
Wnt2
Wnt2B2
Wnt3
Wnt3A
Wnt4
Wnt5A
Wnt5B
Wnt6
Wnt7A
Wnt7B
Wnt8A
Wnt8B
Wnt9A
Wnt9B
Wnt10A
Wnt10B
Wnt11
Wnt16
Empty Vector
H.
Control CM + Compound Library
Pyrvinium pamoate
BML-284
Doxorubicin·HCl
WAY-262611
Forskolin
Niclosamide
BML-285
Bafilomycin A1
PGE2
BIO
Bosutinib
Decitabine
10μM (zScore)
1μM (zScore)
Wnt3a CM + Compound Library
Pyrvinium pamoate
PP2
TWS-119
Niclosamide
Imatinib mesylate
WAY-262611
Hexachlorophene
Bosutinib
Trichostatin A
10μM (zScore)
1μM (zScore)
I.
Control CM
Wnt3a CM
Control
BML-284
Doxorubicin
Forskolin
Control
Trichostatin A
Hexa-chlorophene
Niclosamide

Figure 1

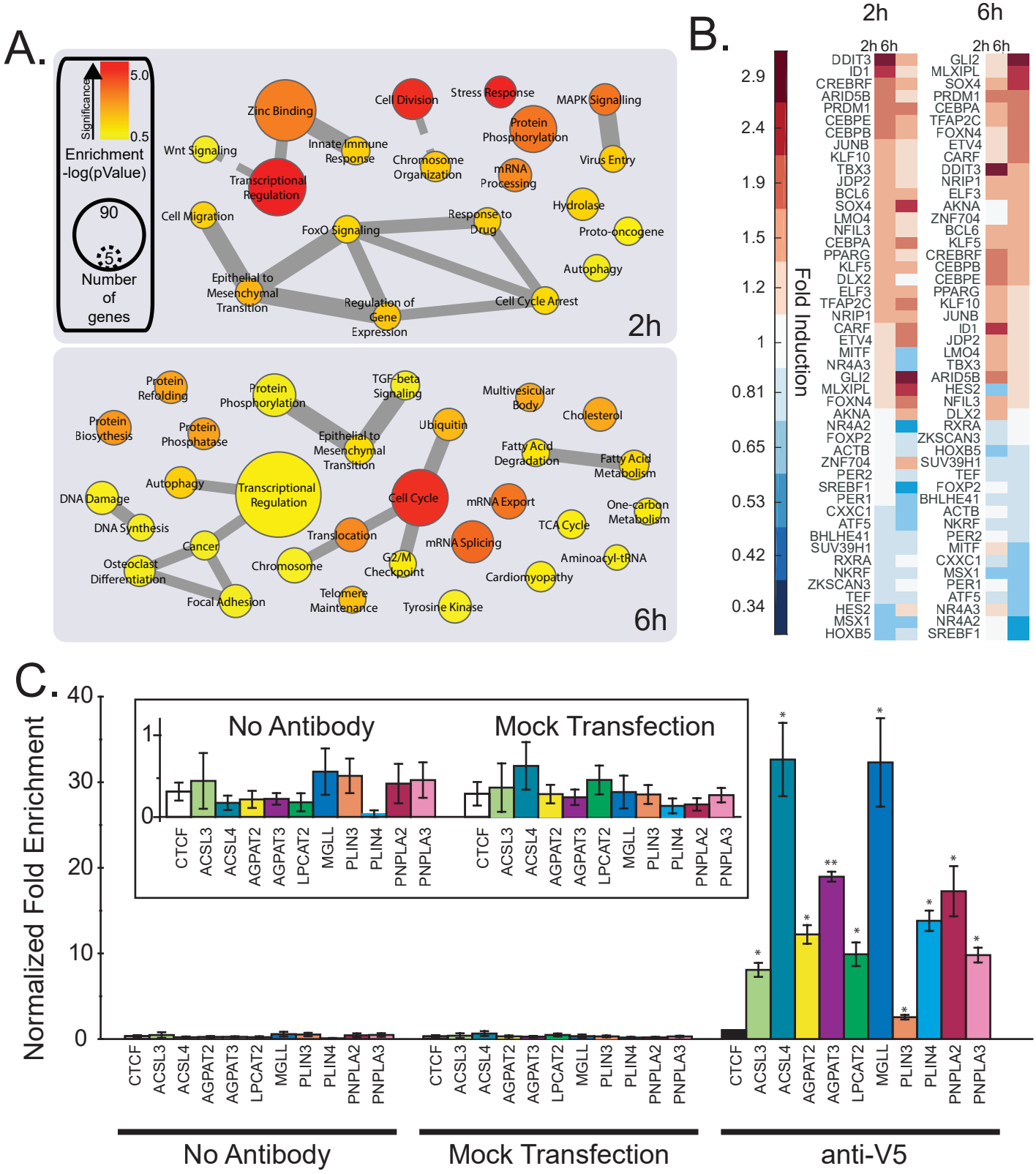
A.
Significance
5.0
0.5
Enrichment
-log(pValue)
90
5
Number
of
genes
Zinc Binding
Cell Division
Stress Response
MAPK Signalling
Wnt Signaling
Innate Immune
Response
Protein
Phosphorylation
Transcriptional
Regulation
Chromosome
Organization
mRNA
Processing
Virus Entry
Cell Migration
Hydrolase
FoxO Signaling
Response to
Drug
Proto-oncogene
Autophagy
Epithelial to
Mesenchymal
Transition
Regulation of
Gene
Expression
Cell Cycle Arrest
2h
Protein
Refolding
Protein
Phosphorylation
TGF-beta
Signaling
Multivesicular
Body
Protein
Biosythesis
Protein
Phosphatase
Ubiquitin
Cholesterol
Epithelial to
Mesenchymal
Transition
Fatty Acid
Degradation
Fatty Acid
Metabolism
Autophagy
Transcriptional
Regulation
Cell Cycle
mRNA Export
DNA Damage
One-carbon
Metabolism
DNA Synthesis
Translocation
TCA Cycle
Cancer
mRNA Splicing
Osteoclast
Differentiation
Chromosome
G2/M
Checkpoint
Aminoacyl-tRNA
Cardiomyopathy
Telomere
Maintenance
Tyrosine Kinase
Focal Adhesion
6h
B.
2h
6h
2h 6h
2h 6h
Fold Induction
2.9
2.4
1.9
1.5
1.2
1
0.81
0.65
0.53
0.42
0.34
DDIT3
ID1
CREBRF
ARID5B
PRDM1
CEBPE
CEBPB
JUNB
KLF10
TBX3
JDP2
BCL6
SOX4
LMO4
NFIL3
CEBPA
PPARG
KLF5
DLX2
ELF3
TFAP2C
NRIP1
CARF
ETV4
MITF
NR4A3
GLI2
MLXIPL
FOXN4
AKNA
NR4A2
FOXP2
ACTB
ZNF704
PER2
SREBF1
PER1
CXXC1
ATF5
BHLHE41
SUV39H1
RXRA
NKRF
ZKSCAN3
TEF
HES2
MSX1
HOXB5
GLI2
MLXIPL
SOX4
PRDM1
CEBPA
TFAP2C
FOXN4
ETV4
CARF
DDIT3
NRIP1
ELF3
AKNA
ZNF704
BCL6
KLF5
CREBRF
CEBPB
CEBPE
PPARG
KLF10
JUNB
ID1
JDP2
LMO4
TBX3
ARID5B
HES2
NFIL3
DLX2
RXRA
ZKSCAN3
HOXB5
SUV39H1
TEF
FOXP2
BHLHE41
ACTB
NKRF
PER2
MITF
CXXC1
MSX1
PER1
ATF5
NR4A3
NR4A2
SREBF1
C.
Normalized Fold Enrichment
40
30
20
10
0
No Antibody
Mock Transfection
1
0
CTCF
ACSL3
ACSL4
AGPAT2
AGPAT3
LPCAT2
MGLL
PLIN3
PLIN4
PNPLA2
PNPLA3
No Antibody
Mock Transfection
anti-V5

Figure 2

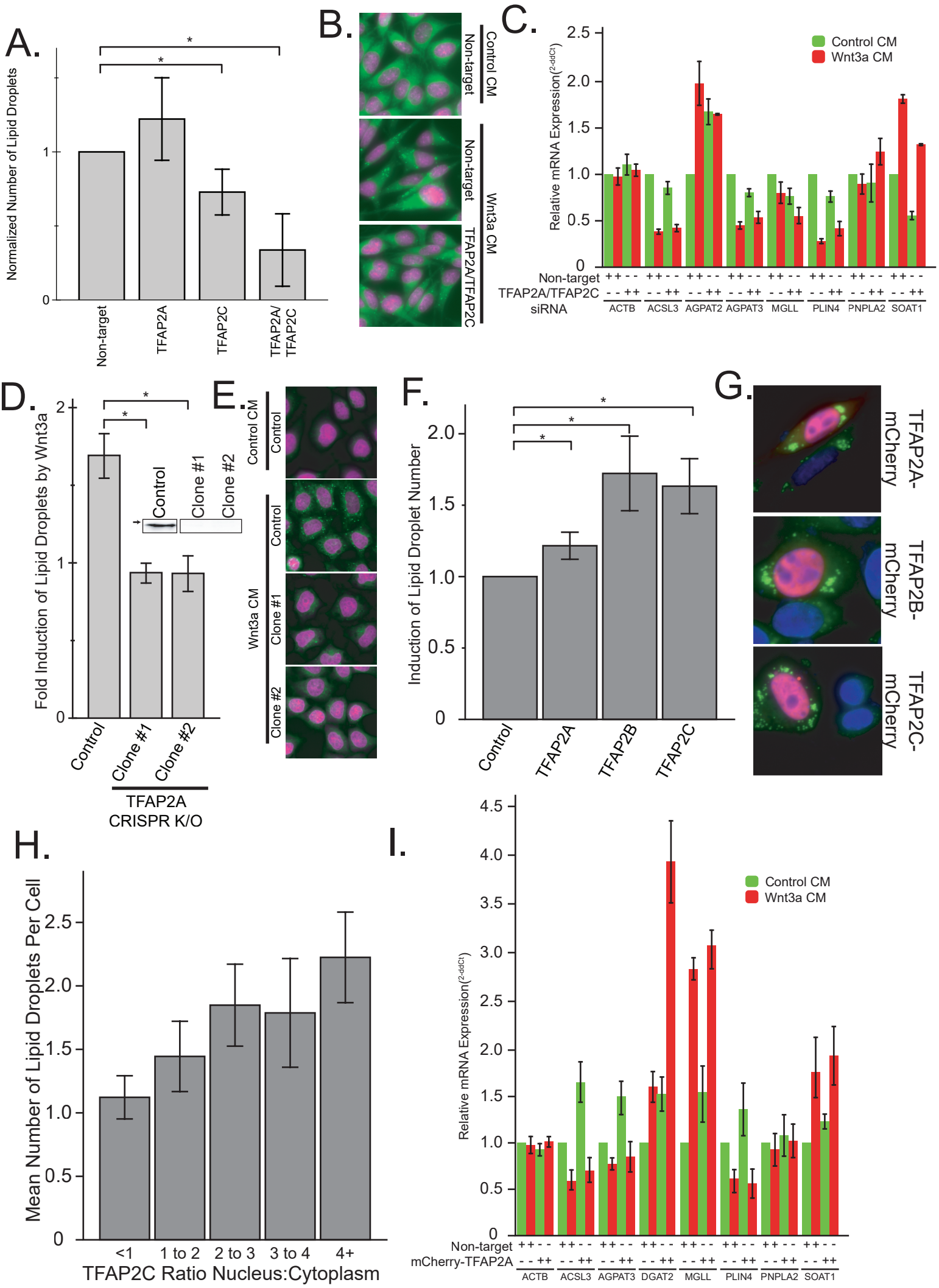
A.
Normalized Number of Lipid Droplets
Non-target
TFAP2A
TFAP2C
TFAP2A/ TFAP2C
B.
Control CM
Non-target
Wnt3a CM
Non-target
TFAP2A/TFAP2C
C.
Relative mRNA Expression(2-ddCt)
Control CM
Wnt3a CM
Non-target
TFAP2A/TFAP2C siRNA
ACTB
ACSL3
AGPAT2
AGPAT3
MGLL
PLIN4
PNPLA2
SOAT1
D.
Fold Induction of Lipid Droplets by Wnt3a
Control
Clone #1
Clone #2
TFAP2A CRISPR K/O
E.
Control CM
Control
Wnt3a CM
Control
Clone #1
Clone #2
F.
Induction of Lipid Droplet Number
Control
TFAP2A
TFAP2B
TFAP2C
G.
TFAP2A-mCherry
TFAP2B-mCherry
TFAP2C-mCherry
H.
Mean Number of Lipid Droplets Per Cell
<1
1 to 2
2 to 3
3 to 4
4+
TFAP2C Ratio Nucleus:Cytoplasm
I.
Relative mRNA Expression(2-ddCt)
Control CM
Wnt3a CM
Non-target
mCherry-TFAP2A
ACTB
ACSL3
AGPAT3
DGAT2
MGLL
PLIN4
PNPLA2
SOAT1

Figure 3

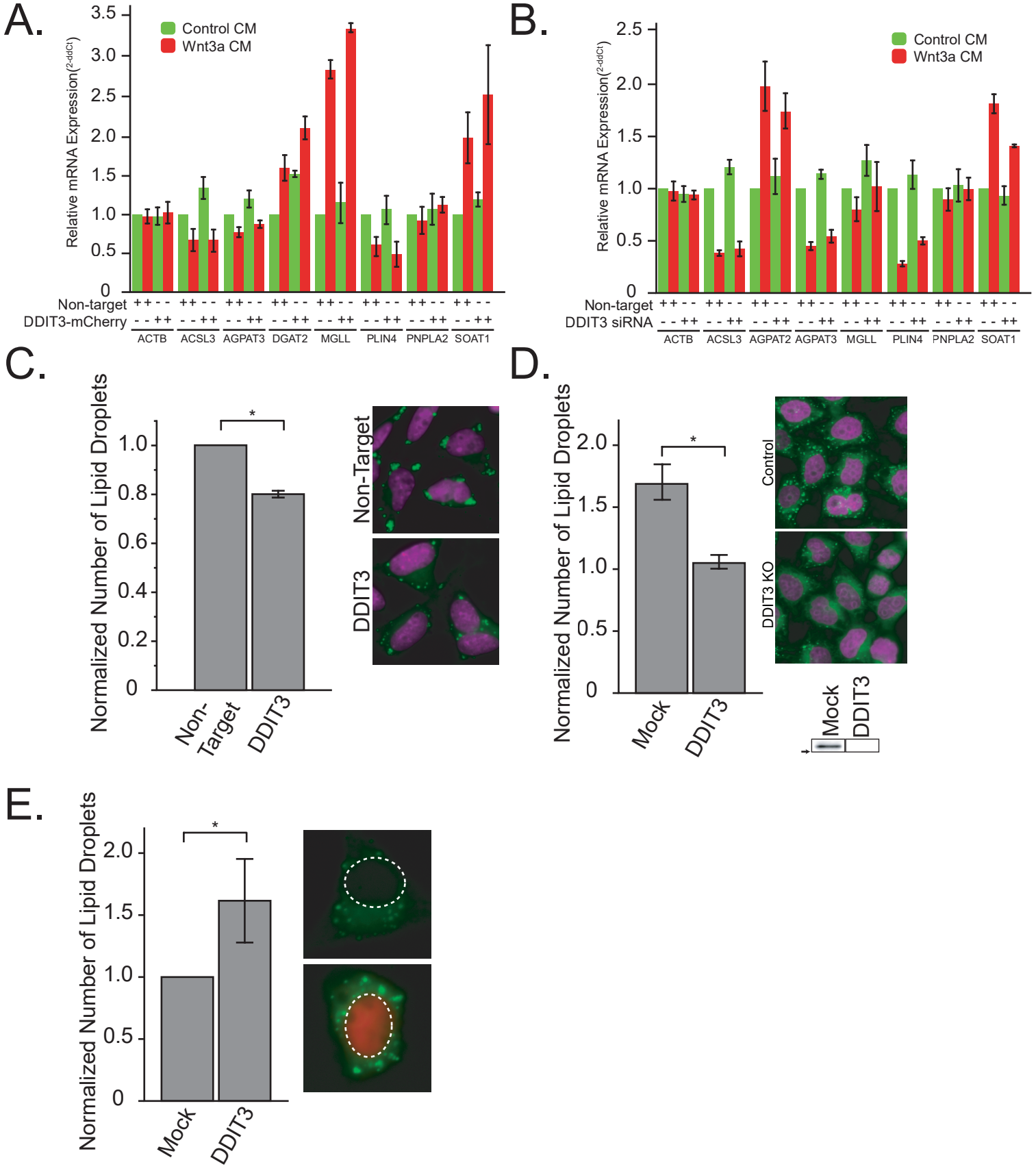
A.
Relative mRNA Expression(2-ddCt)
Control CM
Wnt3a CM
Non-target
DDIT3-mCherry
ACTB
ACSL3
AGPAT3
DGAT2
MGLL
PLIN4
PNPLA2
SOAT1
B.
Relative mRNA Expression(2-ddCt)
Control CM
Wnt3a CM
Non-target
DDIT3 siRNA
ACTB
ACSL3
AGPAT2
AGPAT3
MGLL
PLIN4
PNPLA2
SOAT1
C.
Normalized Number of Lipid Droplets
Non-Target
DDIT3
D.
Normalized Number of Lipid Droplets
Mock
DDIT3
Control
DDIT3 KO
E.
Normalized Number of Lipid Droplets
Mock
DDIT3

Figure 4

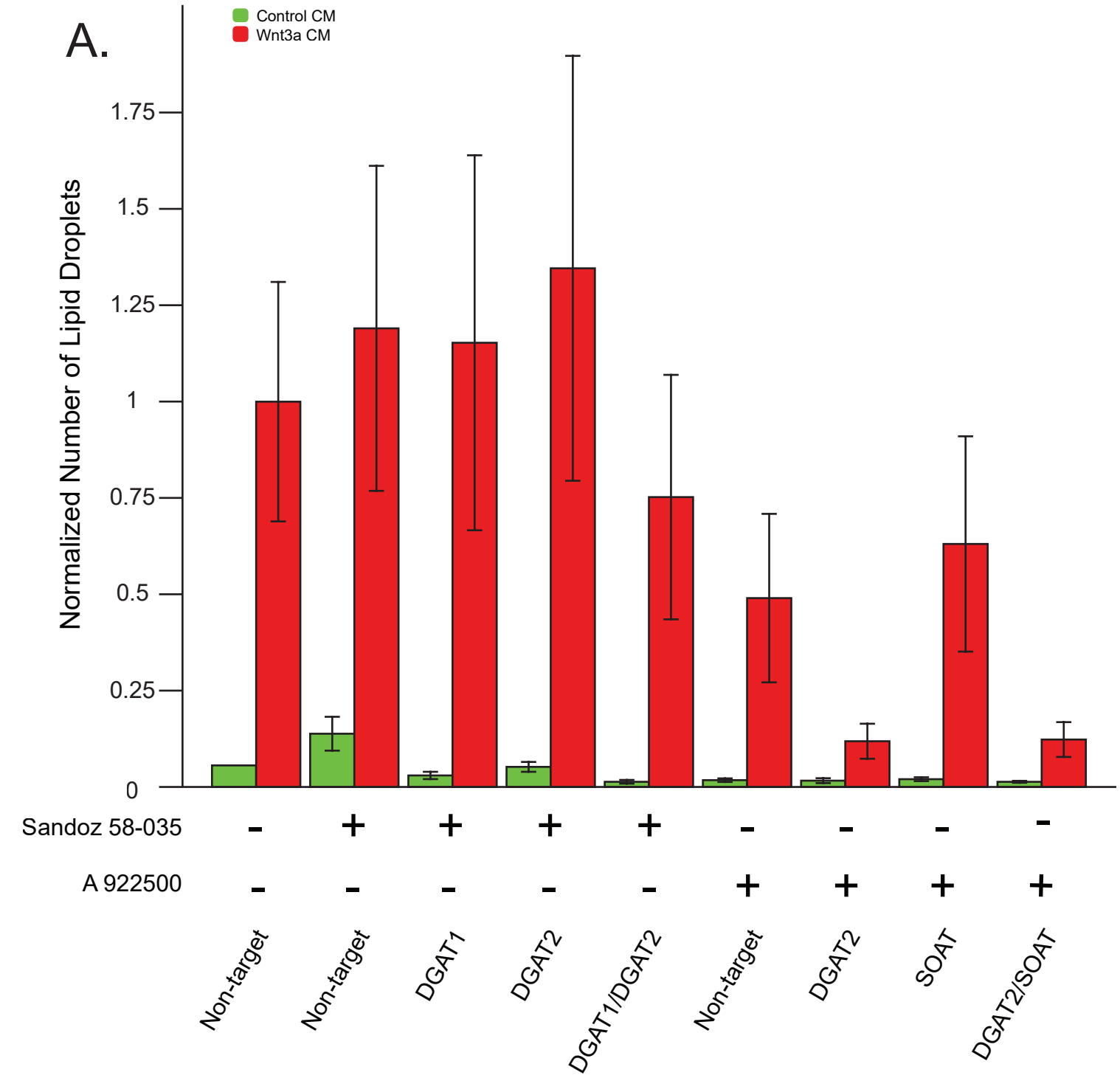

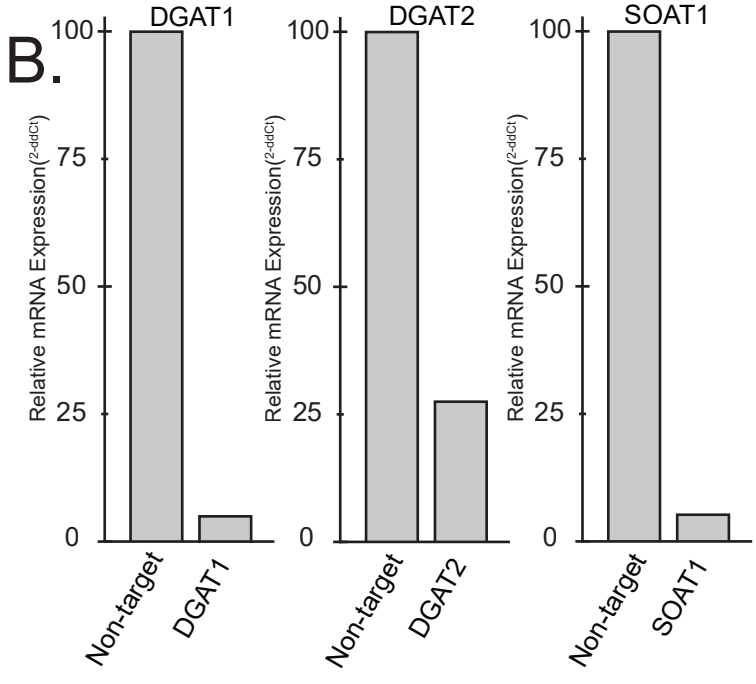

Figure 1 –
Figure Supplement 1

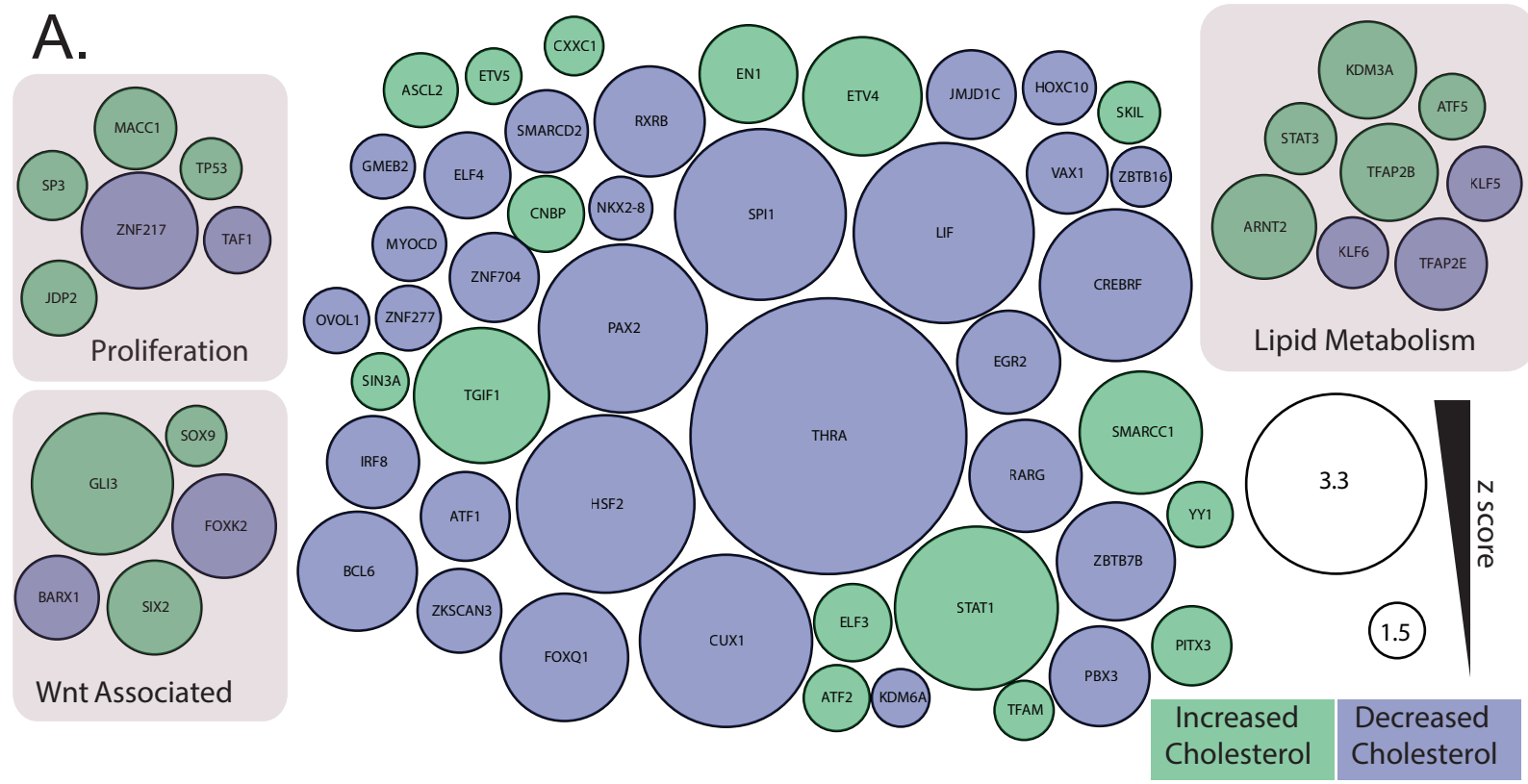

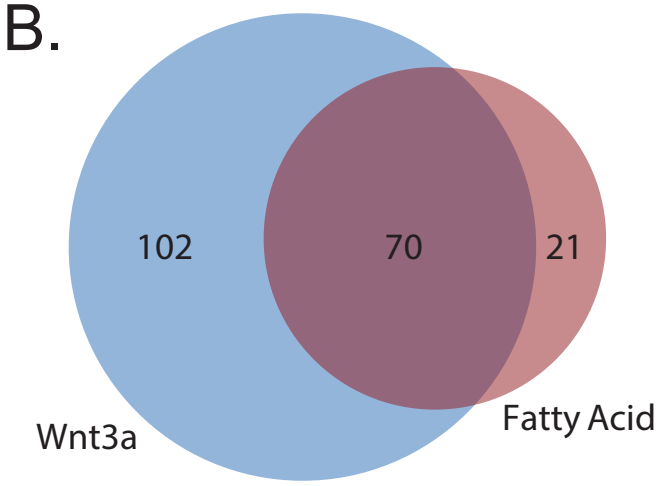

Figure 2 – Figure Supplement 1

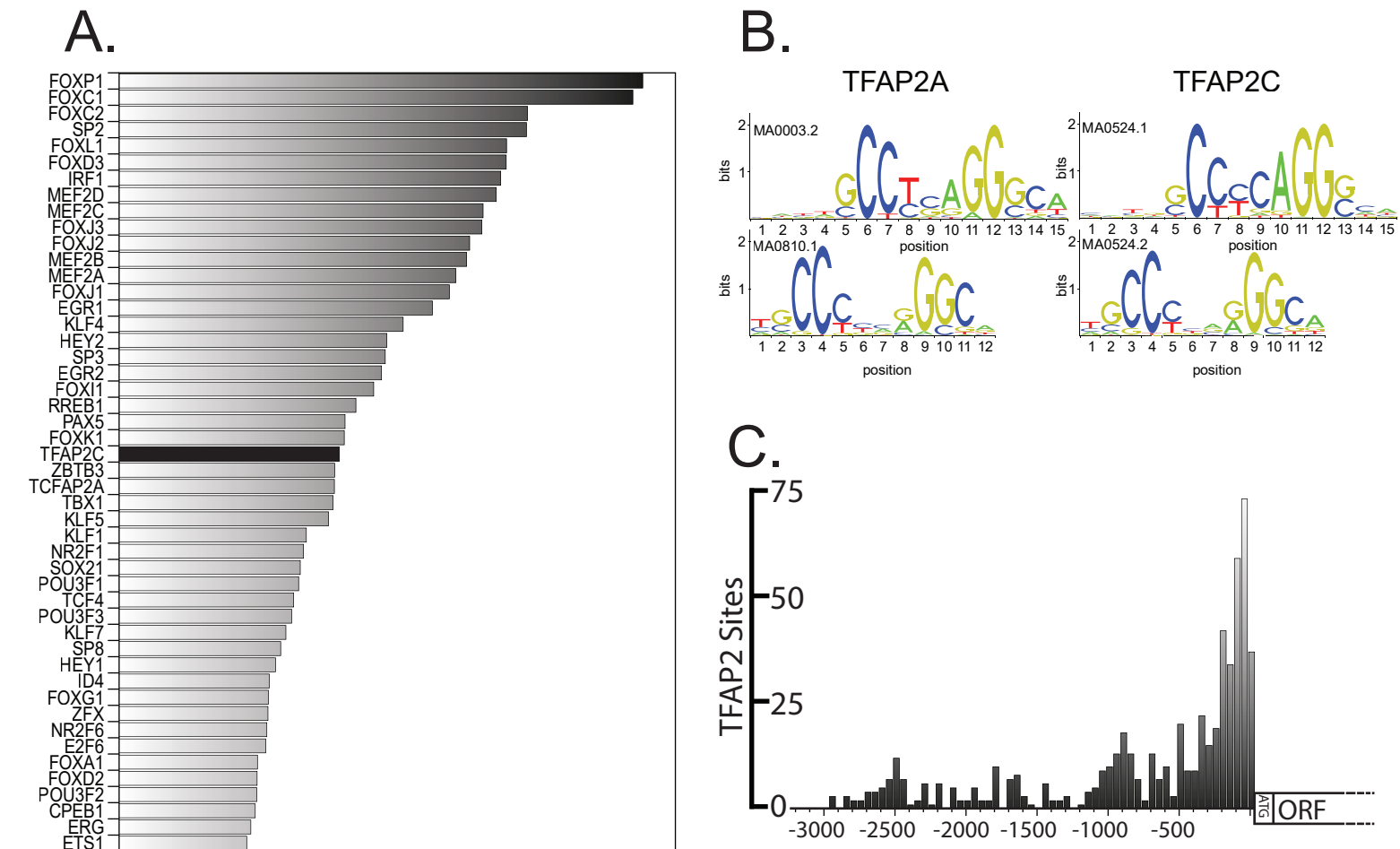

Figure 2 – Figure Supplement 2

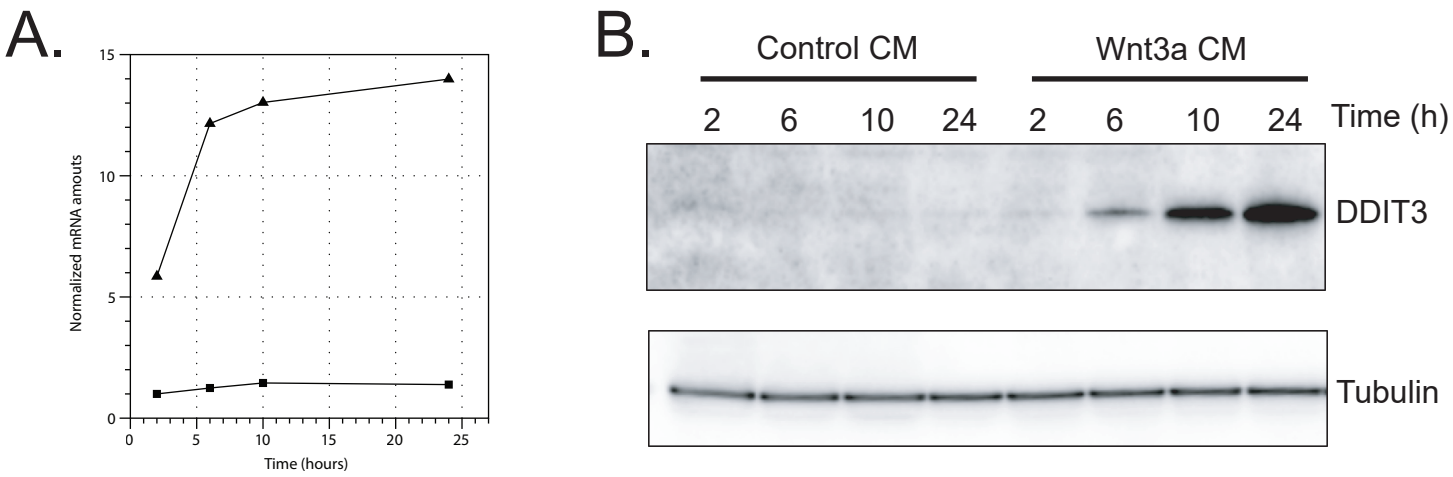

Figure 2 – Figure Supplement 3

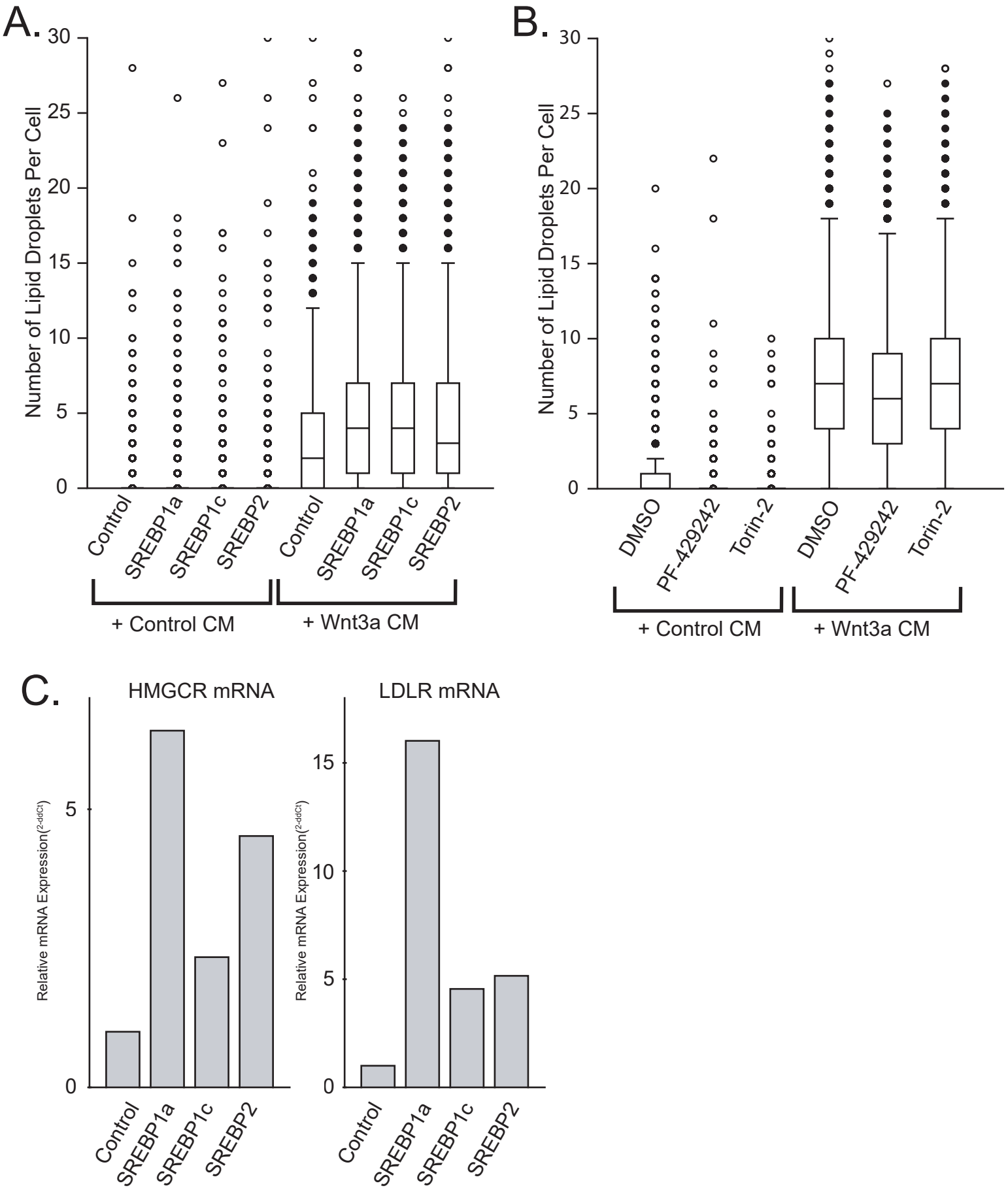

Figure 2 – Figure Supplement 4

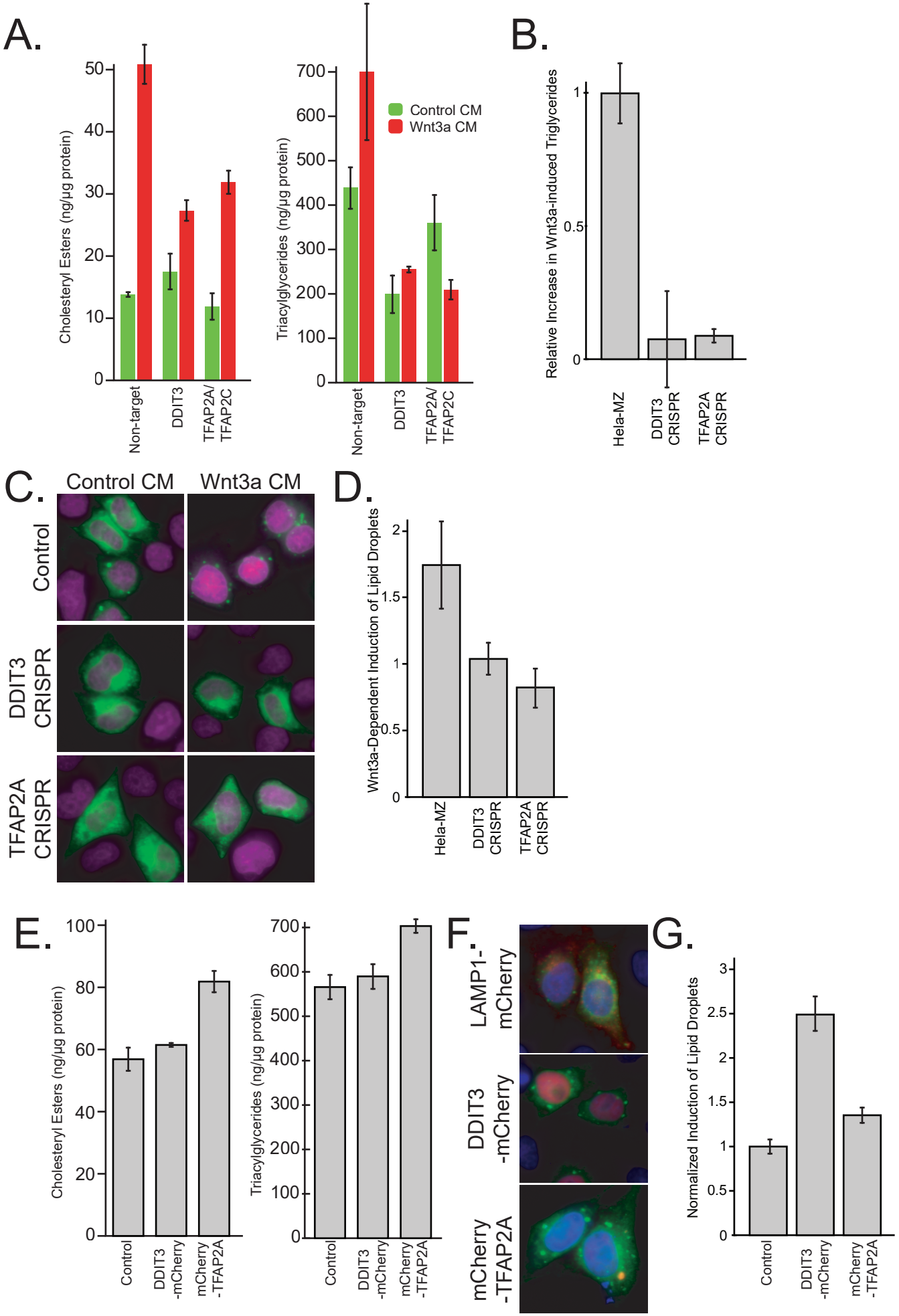

Figure 3 –
Figure Supplement 1

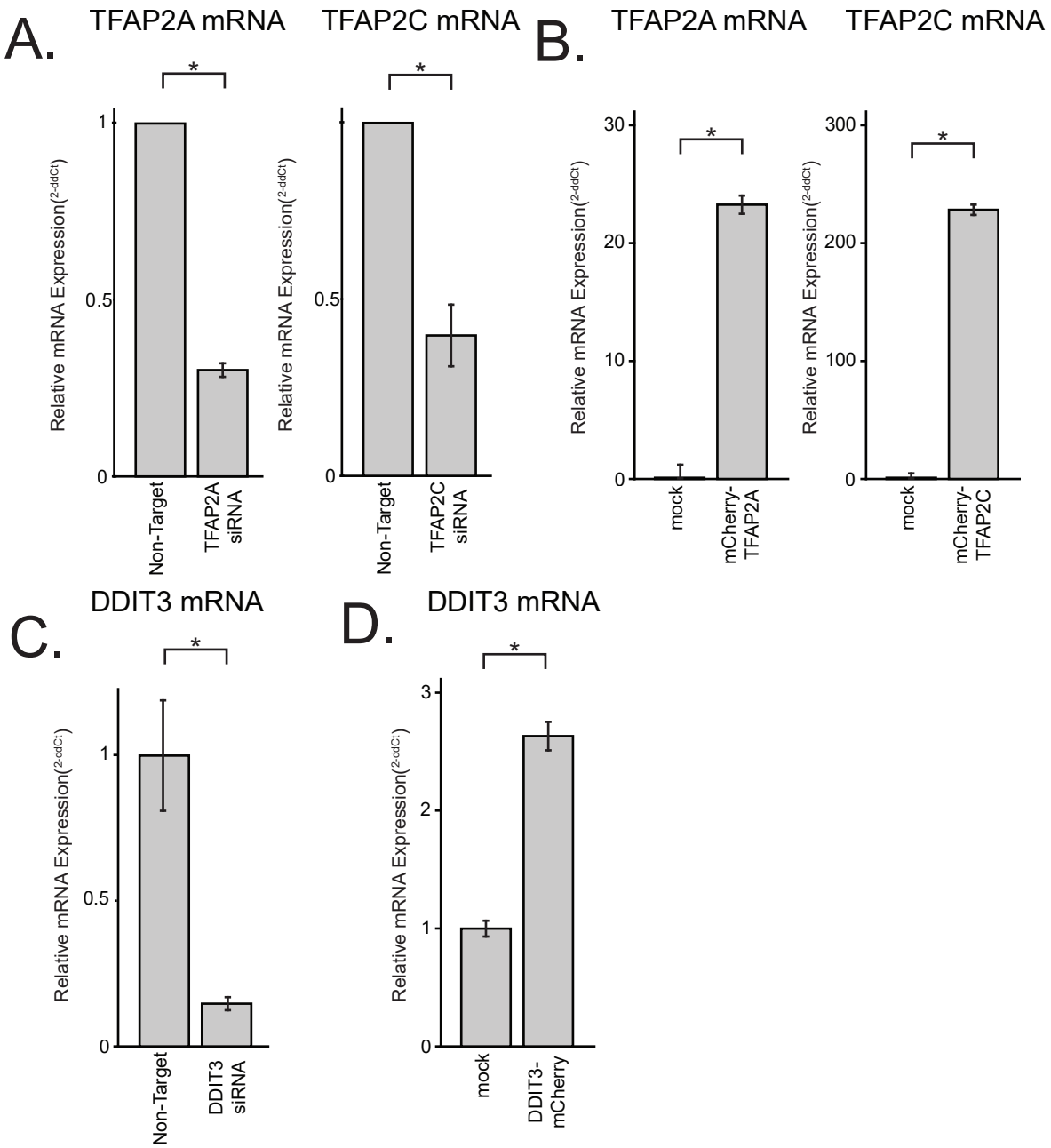

Figure 3 –
Figure Supplement 2

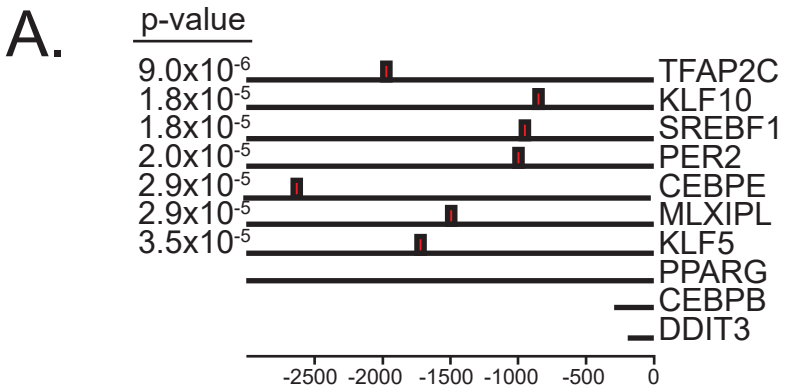

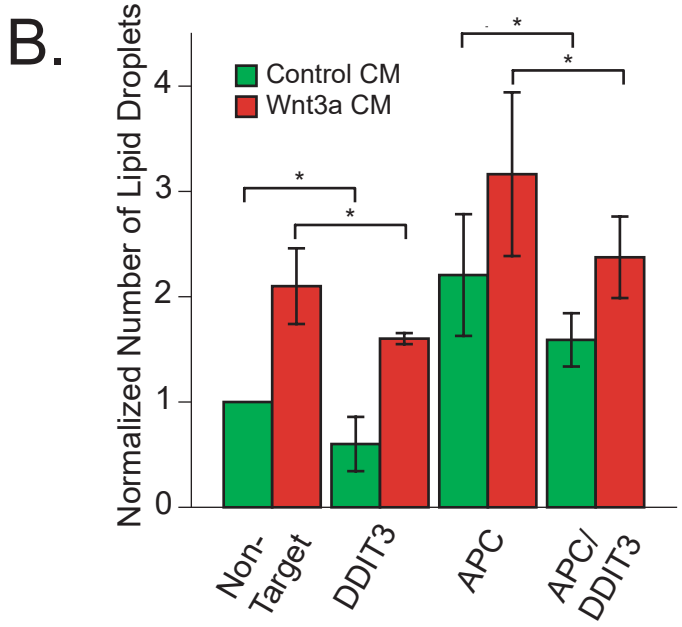

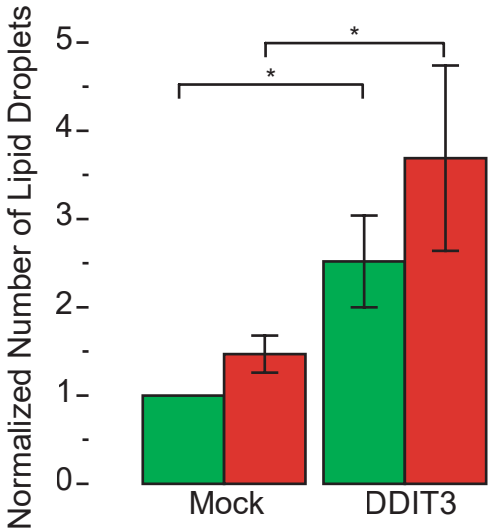

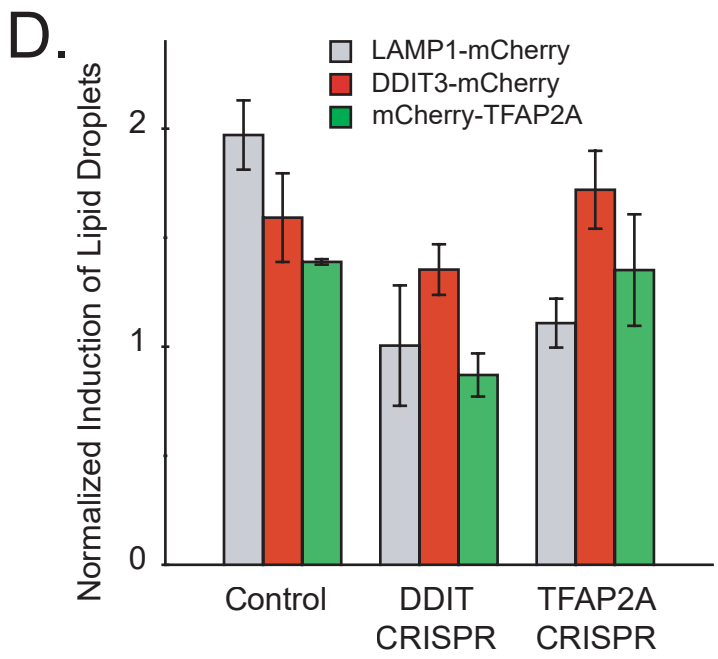

Figure 4 – Figure Supplement 1